

Ozone-Based Technologies in Water and Wastewater Treatment

A. Rodríguez¹ · R. Rosal¹ · J. A. Perdigón-Melón¹ · M. Mezcua² · A. Agüera² · M. D. Hernando¹ · P. Letón¹ · A. R. Fernández-Alba² (✉) · E. García-Calvo¹

¹Department of Chemical Engineering, University of Alcalá,
28871 Alcalá de Henares, Madrid, Spain

²Department of Analytical Chemistry, University of Almería, 04120 Almería, Spain
amadeo@ual.es

| | | |
|----------|---|-----|
| 1 | Fundamentals of Ozonation Processes | 129 |
| 1.1 | The Molecule of Ozone | 129 |
| 1.2 | Solubility of Ozone in Water | 130 |
| 1.3 | Ozone Mass Transfer | 131 |
| 1.4 | Decomposition of Ozone in Water | 134 |
| 1.5 | Ozone Reactions with Organic Compounds | 138 |
| 2 | Ozone Uses in Water Treatment | 140 |
| 2.1 | Precipitation of Oxides | 141 |
| 2.2 | Disinfection of Drinking Water | 143 |
| 2.3 | Natural Water and Wastewater Treatment | 145 |
| 2.4 | Catalytic Ozonation | 153 |
| 2.4.1 | Homogeneous Catalytic Ozonation | 155 |
| 2.4.2 | Catalysis by Metals and Metal Oxides | 156 |
| 2.5 | Applications in the Treatment of Industrial Wastewater | 163 |
| 2.6 | Removal Efficiency of Pharmaceuticals in Wastewater: A Case Study | 166 |
| 3 | Conclusions | 171 |
| | References | 172 |

Abstract Ozone is a strong oxidant that can be used in the potabilization of surface or ground water as well as in wastewater treatment to remove microorganisms, inorganic ions and organic pollutants. The oldest use of ozone is as a biocide in drinking water potabilization. The integral ozone exposure required for a given degree of disinfection can be calculated from the deactivation kinetic constant of the microorganism. Ozone removes iron, manganese and arsenic from water by oxidation to an insoluble form that is further separated by filtration. Both processes require ozone in molecular form, but the removal of organic pollutants that are refractory to other treatments can be possible only by exploiting the indirect radical reactions that take place during ozonation. Ozone decomposes in water, especially when hydrogen peroxide is present, to yield the hydroxyl radical, the strongest oxidizer available in water treatment. Models for the ozonation process are required to adjust the ozone dosing to the desired degree of removal of a given pollutant or an aggregate measure of pollution. Mineralization, defined as the removal of organic carbon, has been accomplished in wastewaters from urban and domestic treatment plants. The results show that the logarithmic decrease of TOC as a function of the integral ozone exposure usually presents two zones with different kinetic parameters.

Among advanced oxidation processes, a promising alternative currently under development is the use of ozone in combination with solid catalysts. The mechanism of catalytic ozonation is not clear, but in the case of metal oxides, the adsorption of ozone or organic compounds on Lewis acid sites is only possible near the point of zero charge of the surface. Activated carbon seems to behave as an initiator of ozone decomposition, a role that may also occur with other types of catalysts. Some results on the mineralization of water with the drugs naproxen (non-steroidal anti-inflammatory) and carbamazepine (anticonvulsant) are presented using titanium dioxide as catalyst.

Keywords Advanced oxidation processes · Disinfection · Kinetic models · Ozonation · Solid catalysts

Abbreviations

| | |
|----------------------------|---|
| a | Specific gas–liquid interfacial area [m^{-1}] |
| Alk | Alkalinity [$\text{mg CaCO}_3 \text{ L}^{-1}$] |
| c_A | Concentration of a given compound [M] |
| C_{O_3} | Concentration of dissolved ozone in water [M] |
| $C_{\text{O}_3}^*$ | Equilibrium concentration of dissolved ozone in water [M] |
| c_s | Bulk concentration of catalyst [kg m^{-3}] |
| c_t | Concentration of surface sites of catalyst [mol kg^{-1}] |
| ct_{O_3}, ct_{10} | Concentration–time exposure parameter for ozone [M s] |
| d_b | Bubble diameter [m] |
| D_{O_2} | Diffusivity of oxygen [$\text{m}^2 \text{ s}^{-1}$] |
| D_{O_3} | Diffusivity of ozone [$\text{m}^2 \text{ s}^{-1}$] |
| E | Enhancement factor |
| Ha | Hatta number |
| H_e | Henry's law constant [atm mole fraction $^{-1}$] |
| i | Ionic strength [M^{-1}] |
| k_1, k_2 | Rate constants for the catalytic decomposition of ozone [$\text{m}^3 \text{ kg}^{-1} \text{ s}^{-1}$] |
| k_a | Kinetic constant of adsorption [$\text{L kg}_{\text{cat}}^{-1} \text{ s}^{-1}$] |
| k_{-a} | Kinetic constant of desorption [$\text{mol kg}_{\text{cat}}^{-1} \text{ s}^{-1}$] |
| k_c | Kinetic constant of catalytic ozonation [$\text{L kg}_{\text{cat}}^{-1} \text{ s}^{-1}$] |
| k_d | Kinetic constant of ozone decomposition [units depending on the order of reaction] |
| k_D, k_{D_i} | Kinetic constants for direct reaction with ozone [$\text{L mol}^{-1} \text{ s}^{-1}$] |
| $k_{\text{HO}\cdot}$ | Kinetic constant for reactions with hydroxyl radical [$\text{L mol}^{-1} \text{ s}^{-1}$] |
| k_{HO^-} | Kinetic constants of the hydroxide initiation of ozone decomposition [$\text{M}^{-1} \text{ s}^{-1}$] |
| $k_{\text{HO}_2^-}$ | Kinetic constants of the hydroperoxide initiation of ozone decomposition [$\text{M}^{-1} \text{ s}^{-1}$] |
| k_L | Liquid phase individual mass transfer coefficient [m s^{-1}] |
| $k_{L,a}$ | Volumetric mass transfer coefficient [s^{-1}] |
| k_N | Kinetic constant for microorganism deactivation [$\text{M}^{-1} \text{ s}^{-1}$] |
| k_o | Kinetic constant of the surface oxidation process [$\text{L kg}_{\text{cat}}^{-1} \text{ s}^{-1}$] |
| k_{O_3} | Kinetic constant for direct reaction with ozone [$\text{L mol}^{-1} \text{ s}^{-1}$] |
| k_t | Kinetic constant of termination reactions [$\text{L mol}^{-1} \text{ s}^{-1}$] |
| K_a | Adsorption equilibrium constant [L mol^{-1}] |
| K_{ox} | Equilibrium constant for the surface oxidation process [L mol^{-1}] |
| N_{O_3} | Absorption rate or flux of ozone [$\text{mol m}^{-2} \text{ s}^{-1}$] |
| pH_{PZC} | pH of the point of zero charge of a surface |

| | |
|------------------|---|
| P_{O_3} | Partial pressure of ozone in gas [Pa] |
| r_d | Rate of ozone decomposition [$\text{mol m}^{-3} \text{s}^{-1}$] |
| R | Kinetic constant for TOC removal during ozonation [$\text{L mol}^{-1} \text{s}^{-1}$] |
| R_{ct} | Hydroxyl ozone ratio defined by Eq. 29 |
| Sc | Schmidt number [$\mu_L \rho_L^{-1} D_{O_3}^{-1}$] |
| TOC | Total organic carbon [mg L^{-1}] |
| TOC_c | Organic carbon refractory to ozonation [mg L^{-1}] |
| TOC_c^* | Organic carbon in oxalate, acetate and formiate [mg L^{-1}] |
| TOC_o | Initial total organic carbon [mg L^{-1}] |
| TOD | Total ozone dose transferred [mol L^{-1}] |
| u_g | Superficial gas velocity [m s^{-1}] |
| X | Ozone dose transfer at the beginning of the ozonation [mol L^{-1}] |
| z | Stoichiometric coefficient |

Greek letters

| | |
|-----------------|---|
| ε_g | Gas holdup |
| μ_L | Liquid viscosity [$\text{kg m}^{-1} \text{s}^{-1}$] |
| ρ_L | Liquid density [kg m^{-3}] |
| σ_L | Surface tension [N m^{-1}] |
| τ | Hydraulic retention time [s] |
| θ | Unit fraction of catalyst occupied sites |

1 Fundamentals of Ozonation Processes

1.1 The Molecule of Ozone

Ozone is a bluish coloured gas with a boiling point of 161.3 K (-111.9°C) and a melting point of 80.7 K (-192.5°C). Mixtures of ozone and oxygen with more than 20% ozone become explosive. In practice, the risk of explosion does not exist because corona discharge commercial ozone generators produce much lower concentrations.

From microwave spectroscopy, it has been shown that the molecule of ozone has an O–O distance of 127.2 pm and an O–O–O angle of 116.78° . The structure of the ozone molecule has been represented by resonance theory by two main equal weighting open structures plus a cyclic form revealed by the electron diffraction method (Fig. 1).

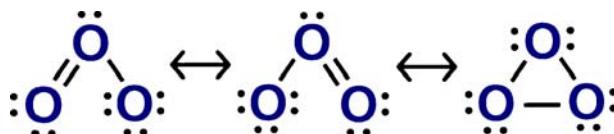


Fig. 1 Resonance structures for the molecule of ozone

Table 1 Oxidation potential for common oxidants referred to a normal hydrogen electrode

| Oxidant | Potential E^0 (V, 25 °C) |
|-------------------|----------------------------|
| Fluoride | 3.06 |
| Hydroxyl radical | 2.80 |
| Atomic oxygen | 2.42 |
| Ozone | 2.07 |
| Hydrogen peroxide | 1.78 |
| Permanganate | 1.68 |
| Chlorine dioxide | 1.57 |
| Hypochlorous acid | 1.49 |
| Chlorine | 1.36 |
| Oxygen | 1.23 |

The central atom in the open structures forms an sp^2 hybridization with one lone pair and positive charge that explains the strong electrophilic behaviour of the molecule. Ozone has a dipole moment of 0.5337 D, a consequence of the electron density of the open structures that strongly influences the chemistry of ozone. Ozone is a very reactive molecule, with a redox oxidation potential of 2.07 V. In fact it is one of the strongest oxidizers available for water treatment (Table 1).

1.2

Solubility of Ozone in Water

The rate and extent of oxidation/mineralization of water pollutants depends on the concentration of dissolved ozone, C_{O_3} . It is, therefore, an essential parameter in the design of water treatment facilities. The ozone mass balance in a volume element of aqueous phase during an isothermal ozonation process controlled by the chemical step is shown in Eq. 1. The value of C_{O_3} is determined by the ozone solubility in water, $C_{O_3}^*$, the volumetric transfer coefficient, $k_L a$, and the ozone decomposition kinetic constant, k_d , due to reactions between ozone and water and the compound dissolved in it:

$$\frac{dC_{O_3}}{dt} = k_L a (C_{O_3}^* - C_{O_3}) - k_d C_{O_3}^n. \quad (1)$$

At low pressure, ozone is only slightly soluble in water and if ideal gas behaviour and a negligible ozone transfer resistance in the gas phase are assumed, the relationship between the partial pressure of ozone, P_{O_3} , and its solubility in water can be expressed by Henry's law:

$$P_{O_3} = C_{O_3}^* H_e. \quad (2)$$

Due to decomposition of ozone in water, the experimental determination of parameters from Eq. 1 is not easy. It is usual to calculate $C_{O_3}^*$ by means of Eq. 2 taking H_e values from published correlations, such as those of Andreozzi et al. and Rischbieter et al. [1, 2]:

$$\log(H_e) = A - \frac{B}{T}, \quad (3)$$

where A and B are parameters that depend on the ionic strength of the solution; Roth and Sullivan [3], where H_e (atm mole fraction⁻¹) is expressed as a function of temperature and pH of water:

$$H_e = 3.84 \times 10^7 C_{OH^-}^{0.035} \exp\left(-\frac{2428}{T}\right), \quad (4)$$

or Sotelo et al. [4], in which H_e (kPa mole fraction⁻¹) depends on temperature, pH, ionic strength (i) and type of salt dissolved in water:

$$H_e = 1.03 \times 10^9 C_{OH^-}^{0.012} \exp\left(-\frac{2118}{T}\right) \exp(0.96 i). \quad (5)$$

Equation 5 corresponds to sodium phosphate solutions and $0 \leq T \leq 20$ °C, $2 \leq \text{pH} \leq 8.5$, and $10^{-3} \text{ M} \leq i \leq 10^{-1} \text{ M}$. The $C_{O_3}^*$ values estimated from these or similar equations are close to the ozone solubility values in real wastewater, although in cases where an important deviation between the estimated and real solubility values is expected, the Henry's law constant must be experimentally measured [5].

1.3

Ozone Mass Transfer

The absorption rate of ozone in water, N_{O_3} , can be expressed as:

$$N_{O_3} a = k_L a (C_{O_3}^* - C_{O_3}), \quad (6)$$

where k_L is the ozone mass transfer coefficient and a the specific gas-liquid interfacial surface inside the ozonation reactor. As indicated in the preceding section, the concentration of dissolved ozone depends also on the rate of ozone decomposition, r_d :

$$r_d = k_d C_{O_3}^n. \quad (7)$$

Expressions similar to Eq. 7 permit an easy estimation of the ozone consumption rate in complex systems, such as those that occur in the ozonation of wastewater (see Sect. 2.4). The parameter k_d in Eq. 7 is not a real kinetic constant because, besides temperature, its value depends on the properties of the water matrix: organic and inorganic matter dissolved, pH, alkalinity and ionic strength.

The ozonation kinetics may be controlled either by physical absorption or by chemical reaction. The value of the Hatta number gives a rule to determine the rate-controlling process for a set of given conditions [6]. The Hatta number is calculated with the values of k_L and k_d and assuming the double film model of Lewis–Whitman [7]:

$$Ha = \frac{\sqrt{\left(\frac{2}{n+1}\right) D_{O_3} k_d C_{O_3}^{n-1}}}{k_L}, \quad (8)$$

where D_{O_3} is the ozone diffusivity in water and n the ozone decomposition kinetic order. For $Ha < 0.3$, the rate of ozone absorption is higher than the ozone decomposition rate and, therefore, chemical kinetics controls the ozonation process (Eq. 1). Operation conditions should guarantee that the process is controlled by the chemical reaction step in order to provide a maximum flow of oxidant. At operational conditions with $Ha > 0.3$ values, the ozonation decomposition rate is so high that the concentration of ozone in water cannot be measured and the absorption step controls the overall ozonation process. In these cases, the ozone transfer model must take into account the contribution of the chemical reaction to the absorption expressed by the enhancement factor (E), either calculated by the general approach [7, 8] or by means of experiments [9]:

$$N_{O_3} a = k_L a C_{O_3}^* E. \quad (9)$$

The diffusivity of ozone can be calculated by the Wilke–Chang type correlation of Hayduk et al. or by means of ozone-specific expressions, such as those proposed by Matrosov et al. ($A = 4.27 \times 10^{-10}$) or Jonson and Davis ($A = 5.9 \times 10^{-10}$) with the following expression [10]:

$$D_{O_3} = A \frac{T}{\mu_L}, \quad (10)$$

where D_{O_3} is in $m^2 s^{-1}$, T in K and μ_L , the solution viscosity, in poise. The mass transfer coefficient, k_L , can be estimated from equations such as that proposed by van Dierendonck for stirred tanks in which μ_L and ρ_L , the viscosity and density of the aqueous solution, are expressed in SI units:

$$k_L = 0.42 \sqrt[3]{\frac{\mu_L g}{\rho_L}} Sc^{-0.5}. \quad (11)$$

In bubble columns and for bubble sizes $d_b < 2$ mm, Calderbank proposed the same equation to estimate k_L and Eq. 12 for bubbles with $d_b > 2$ mm:

$$k_L = k_{L(d_b=2 \text{ mm})} 500 d_b. \quad (12)$$

The bubble diameter can be estimated from the operation parameters u_g (superficial gas velocity) and ε_g (gas holdup into the column) and the liquid-

phase properties ρ_L (density) and σ_L (surface tension):

$$\frac{6(1 - \varepsilon_g)}{d_b} = 2 \left(\frac{\rho_L g}{\sigma_L} \right)^{0.5} \frac{u_g}{\left(\frac{\sigma_L g}{\rho_L} \right)^{0.25}} \quad (13)$$

If all bubbles are spheres with the same size, a can be calculated by:

$$a = \frac{6\varepsilon_g}{d_b} \quad (14)$$

Although in Eqs. 10–14 the contribution of pollutants present in wastewater has not been taken into account, the values of k_L , D_{O_3} and a obtained from them will be used to characterize the transfer phenomenon taking place in ozonation processes. According to Beltrán [11], k_L , D_{O_3} and a can be experimentally determined in the wastewater where ozonation processes take place provided the appropriate kinetic regime is chosen. The experiments performed to determine $k_L a$ and k_d consist in bubbling a continuous gas flow containing ozone through the wastewater in a stirred tank or bubble column where ozonation takes place. Figure 2 shows the concentration of dissolved ozone during the ozonation of a wastewater (Table 5, D070208) from the secondary clarification of a municipal wastewater treatment facility. The experiment was carried out at 25 °C in a 5-L stirred tank agitated at 1000 rpm with a four-blade turbine. The gas, a mixture of ozone and oxygen with a 45.9 g Nm⁻³ ozone concentration, was bubbled at a rate of 0.36 Nm³ h⁻¹. During the experiment the pH was in the range 8.04–8.25. Three different zones can be appreciated in Fig. 2. Zone I is characterized by a strong increase in ozone dissolved concentration and is followed by zone II, where the ozone concentration reaches a stationary value, C_{O_3s} . In zone III the concentration of ozone decays after stopping the gas flow.

Assuming that the decomposition of ozone follows first-order kinetics, Eq. 1 applied to zones II and III leads to the following expressions:

$$0 = k_L a (C_{O_3}^* - C_{O_3s}) - k_d C_{O_3s} \quad (15)$$

$$\frac{dC_{O_3}}{dt} = -k_d C_{O_3} \quad (16)$$

The integration of Eq. 16 yielded k_d . The solubility of ozone was calculated as indicated in Sect. 1.2 and the value of $k_L a$ was obtained from Eq. 15. The experimental value of $k_L a$ can be up to two or five times higher than the corresponding estimation from literature correlations due to the specific composition of wastewater [5].

For the operational conditions of the experiment that is represented in Fig. 2, the calculated values of $C_{O_3}^*$, $k_L a$ and k_d were 0.247 mM, 0.614 min⁻¹ and 0.139 min⁻¹, respectively. (The equation from Rischbieter et al. ($A = 5.12$, $B = 1230 \text{ K}^{-1}$) was used to determine H_e .)

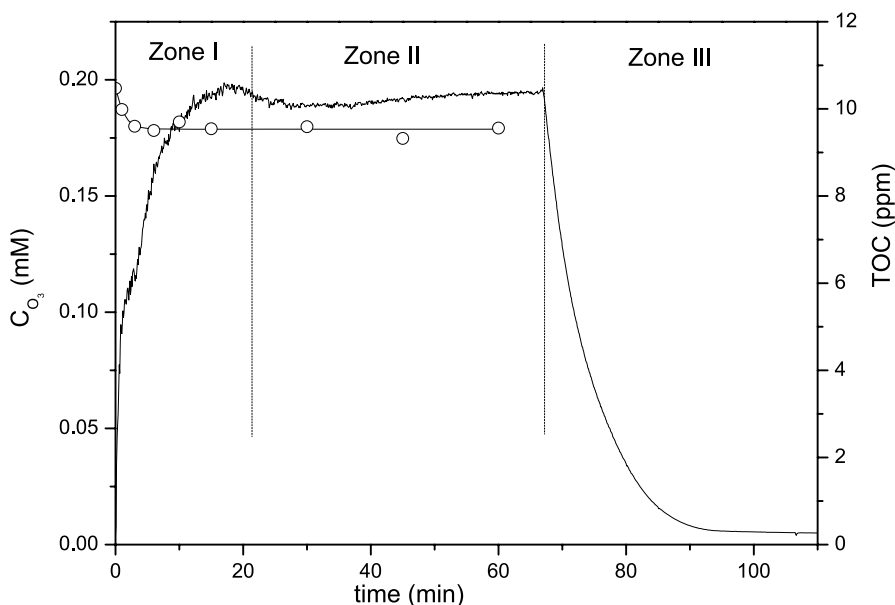


Fig. 2 TOC and C_{O_3} values during the ozonation of D070208 wastewater (Table 5). pH: 8.04–8.25, T : 25 °C, gas flow rate: $0.36 \text{ Nm}^3 \text{ h}^{-1}$, gas ozone concentration: 45.9 g/Nm^3 , $k_{L,a} = 0.614 \text{ min}^{-1}$

The decomposition of ozone in water makes the experimental determination of $k_{L,a}$ complex. To overcome this, and taking the surface renewable theories into account, the ozone mass transfer coefficient can be based on the corresponding value of some less reactive compound such as oxygen at the same pressure and temperature:

$$(k_{L,a})_{O_3} = (k_{L,a})_{O_2} \left(\frac{D_{O_2}}{D_{O_3}} \right)^{0.5} \quad (17)$$

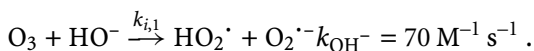
1.4

Decomposition of Ozone in Water

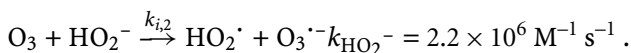
Ozone in aqueous solution decomposes through a complex mechanism initiated by reaction with a hydroxide ion and followed by formation of several radical oxidizing species, such as HO, HO₂ and HO₃. The structures of ozone and HO_x in liquid water remain uncertain. Chalmet and Ruiz-López [12] combined quantum and classical computer simulations and showed that even if ozone undergoes electron polarization, it does not participate in hydrogen bonds with liquid water. In contrast, HO_x form strong hydrogen bonds, being better proton donors but weaker proton acceptors than water. Their electronic and geometrical structures are significantly modified by the solvent, suggest-

ing that water plays a crucial role in oxidation mechanisms initiated by ozone in liquid water.

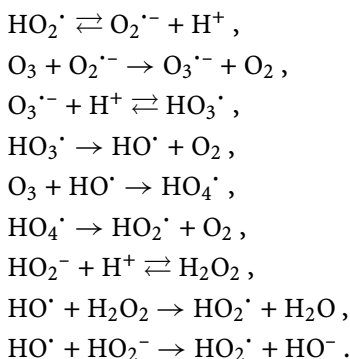
Concerning the mechanism and kinetics of ozone decomposition, the reaction follows a chain process extensively studied by Buhler et al. [13], Staehelin et al. [14], Tomiyasu et al. [15] and Hoigné [16]. In the absence of UV radiation or solid catalysts, the initiation takes place through a reaction between ozone and the hydroxide ion to yield a hydroperoxide (HO_2^\cdot) and a superoxide radical ion ($\text{O}_2^{\cdot-}$):



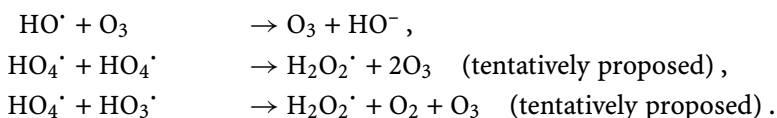
In the presence of hydrogen peroxide, initiation takes place by reaction of ozone with the hydroperoxide ion, HO_2^- , the conjugate base of hydrogen peroxide:



Propagation involves the formation of ozonide radical ion $\text{O}_3^{\cdot-}$, the radical species HO_3^\cdot and HO_4^\cdot and several reactions of hydrogen peroxide, an intermediate product of the degradation chain:



Homogeneous termination takes place by reactions consuming radicals:

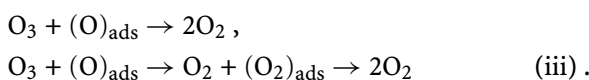


There are a wide variety of compounds able to promote or inhibit the chain-reaction processes. Promoters of the free-radical reaction are substances capable of regenerating the superoxide anion from the hydroxyl radical. Common organic promoters include formic and glyoxylic acids, primary alcohols and humic acids. The inhibitors of the free-radical reaction are compounds capable of consuming hydroxyl radicals without regenerating the superoxide anion. These include bicarbonate and carbonate ions, tertiary alcohols like *tert*-butanol and some humic substances [11, 17].

The formation of hydroxyl radicals from ozone can be enhanced by the presence of solid catalysts. In the case of metal oxides, heterogeneous ozone decomposition is determined by the presence of surface hydroxyl groups acting as Brønsted acid sites. These sites also determine the charge of the surface as a function of pH, and therefore the ion-exchange behaviour of the catalyst. In addition to this, metal oxides have Lewis acid sites that, in an aqueous solution, allow water molecules to coordinate on their surface [18]. The adsorption of ozone requires the displacement of coordinated water and is strongly dependent on the presence of other bases. In the case that a Lewis site is accessible to ozone, the mechanism for its adsorption/decomposition on a catalytic surface would follow a mechanism similar to that used for explaining gas-phase decomposition [19]:



The interaction of the ozone molecule with an oxidized site may yield adsorbed or non-adsorbed oxygen:

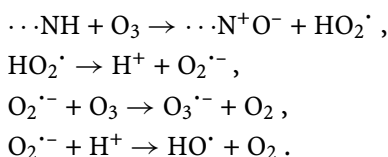


In aqueous solution, the hydroxide ion is expected to act as a strong inhibitor of the adsorption ability of the catalyst by blocking Lewis acid sites. Therefore, the catalytic activity at high pH should proceed by a redox mechanism involving surface hydroxyl groups. Ozone would react with them to yield an ozone anion radical or another active species able to oxidize organic compounds either in solution or on the surface.

Activated carbon is particularly efficient as an initiator in the decomposition reaction of ozone in the liquid phase [20]. The capacity of activated carbon to transform ozone into hydroxyl radicals depends on its surface properties. It has been demonstrated that metal centres, electrons from graphenic layers and basic surface groups like chromene and pyrone are active sites for ozone adsorption [21]. These basic Lewis sites are located at π -electron-rich regions and behave as a Lewis base in aqueous solution [22]:



The molecule of ozone may attack the basic delocalized π -electron system or lone pairs in pyrrolic groups with the generation of hydroxyl radicals [23]:



The generation of radicals from the interaction between ozone and activated carbon has been studied by the R_{ct} methodology using *p*CBA as probe compound [24]. Sánchez-Polo et al. [21] showed that the interaction between ozone and groups on the surface of activated carbon leads to an increase of the concentration of superoxide radical ion enhancing ozone transformation into hydroxyl radicals. As the activity of activated carbon decreased with ozone exposure, it has been suggested that activated carbon does not behave as a true catalyst but rather as a conventional initiator or promoter for the ozone transformation into radicals.

Figure 3 shows the transient response of dissolved ozone concentration after charging a semicontinuous reactor with a catalyst concentration of 0.5 g/L. The mixture of ozone and oxygen was bubbled into the liquid by means of a porous glass disc with a total gas flow of 240 NL/h. The catalysts used were titanium dioxide Degussa P25 and activated carbon (AC). The concentration of ozone in the liquid was measured using a Rosemount 499A OZ ozone amperometric sensor equipped with Pt 100 RTD temperature compensation and checked against the Indigo Colorimetric Method (SM 4500-O₃ B). The signal was continuously monitored by means of a Rosemount 1055 Dual Input Analyzer connected to an Agilent 34970A data acquisition system.

The unsteady-state catalytic decomposition of ozone can be modelled assuming that simultaneous non-catalytic reaction follows a first-order kinetic expression. Ozone was supposed to adsorb on the surface of titanium dioxide,

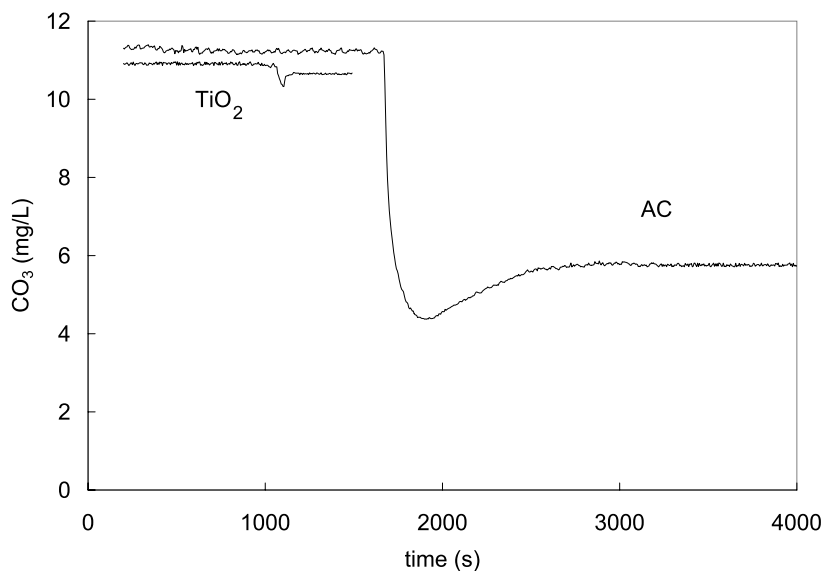


Fig. 3 Transient state decomposition of ozone at 25 °C after introducing 0.5 g/L of TiO₂ and AC while bubbling ozone (40–42 g/Nm³ at 240 NL/h and pH = 5)

so that its decomposition takes place according to the mechanism based on gas-phase reaction and described before. In the absence of data on adsorbed and non-dissociated ozone intermediates, the first reaction can be described as: $O_3 \rightarrow (O)_{\text{ads}} + O_2$. A further ozone molecule reacts with the oxidized site to yield non-adsorbed products. The concentration of ozone can be calculated by solving the following system of differential equations:

$$\frac{dC_{O_3}}{dt} = k_L a E \left(C_{O_3}^* - C_{O_3} \right) - k_1 c_s C_{O_3} (1 - \theta) - k_2 c_s C_{O_3} \theta - k_d C_{O_3}, \quad (18)$$

$$-c_t \frac{d\theta}{dt} = -k_1 C_{O_3} (1 - \theta) + k_2 C_{O_3} \theta, \quad (19)$$

where θ is the fraction of catalyst occupied surface sites, k_1 and k_2 are the rate constants for the catalytic reactions (i + ii) and (iii) and c_s is the bulk concentration of solids. Rosal et al. [25] reported the following kinetic constants at pH = 5 and 20 °C for ozone decomposition on titanium dioxide: $k_1 = 7.21 \times 10^{-3} \pm 3.1 \times 10^{-4} \text{ m}^3 \text{ kg}^{-1} \text{ s}^{-1}$, $k_2 = 2.73 \times 10^{-4} \pm 2.5 \times 10^{-5} \text{ m}^3 \text{ kg}^{-1} \text{ s}^{-1}$ and $k_d = 8.74 \times 10^{-3} \pm 1.3 \times 10^{-4} \text{ s}^{-1}$. Lin et al. [19] compared average rates of decomposition of aqueous ozone, showing that oxides with lower Δh_f exhibit higher activities but always lower than those of noble metals and much lower than those of activated carbon.

Another factor that has been pointed out is the fact that fine catalyst particles may enhance the absorption of ozone by a “shuttle” mechanism involving the physical adsorption of ozone on the surface of particles [26]. For P25 titanium dioxide the maximum enhancement, denoted by E in Eq. 18, represented three times the mass transfer rate of ozone in a particle-free liquid [25].

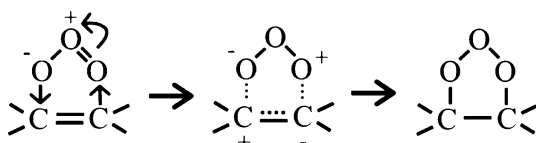
1.5

Ozone Reactions with Organic Compounds

Ozonation may take place by the direct reaction of the ozone molecule with the target compound or by means of hydroxyl radicals produced from the decomposition of ozone in aqueous media. It has already been stated that hydroxyl radicals are strong secondary oxidants produced as a consequence of ozone self-decomposition in water. In practice, both direct and indirect reactions take place simultaneously, but when an oxidation process is specifically designed to enhance the concentration of HO \cdot radicals in a solution, one speaks of an advanced oxidation process (AOP). The data of Acero and von Gunten [27] and Buffle et al. [28, 29] allow some insight into the order of magnitude of the concentration of both oxidants in an ozonation process. These researchers found that the ratio of the concentration of hydroxyl radicals to dissolved ozone ranges from 10^{-6} to 10^{-8} , the former value being encountered in AOP while the latter is typical from the ozonation of drinking water. The hydroxyl concentration during the early stages of ozone

decomposition in water is greatly enhanced by the presence of amines or phenols through the formation of ozonide (O_3^-) or superoxide (O_2^-) radical anions [23].

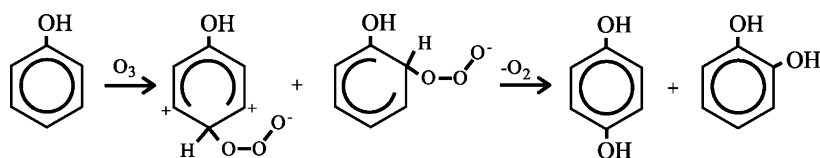
The direct reactions of ozone with organic compounds in aqueous solutions are essentially limited to those taking place with unsaturated and aromatic compounds and are governed by the dipolar structure of the ozone molecule. The 1,3-cycloaddition to unsaturated compounds leads to the formation of a primary ozonide:



In a protonic solution, the primary ozonide decomposes via a zwitterion that yields a hydroperoxide. This three-step process is called the Criegee mechanism.

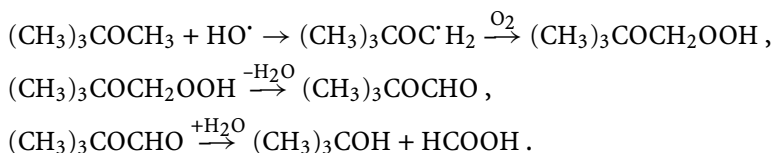


Aromatic compounds do not undergo cycloaddition. Instead, the ozone molecule attacks electrophilic positions in the aromatic ring. Electron-donating groups like $-OH$ or $-NH_2$ induce a high electronic density in the *ortho* and *para* positions and, consequently, in these positions aromatic compounds react actively with ozone. Electron-withdrawing groups such as $-COOH$ deactivate the aromatic ring for the substitution reaction. The reaction is favoured by a resonance of the intermediate. For example, the attack in the *ortho* position of phenol takes place by the following mechanism [30]:

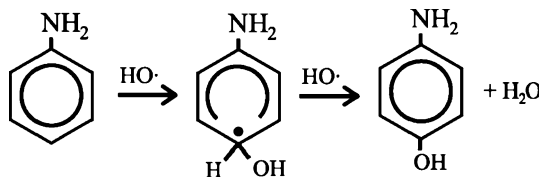


Hydroxyl radicals initiate oxidative degradation by three reactions: hydrogen abstraction, hydroxyl addition and electron transfer. A saturated organic compound may be attacked by a hydroxyl radical and may undergo hydrogen abstraction, a negligible reaction in compounds with aromatic rings and

double bonds [31]. It has been reported that the indirect oxidation of methyl-*tert*-butyl ether starts with the abstraction of an α -hydrogen to form an organic radical, which reacts with oxygen to yield a peroxy radical with a large ($\sim 10^9 \text{ M}^{-1} \text{ s}^{-1}$) second-order rate constant [32]. The peroxy radical can abstract hydrogen to form α -hydroperoxy methyl-*tert*-butyl ether. In aqueous solution, the reaction continues with the hydrolysis of the oxygen–oxygen bond to produce *tert*-butyl formate and, subsequently, formic acid and *tert*-butyl alcohol:



Unsaturated and aromatic compounds undergo hydroxyl addition, a reaction with a very high rate (10^9 – $10^{10} \text{ M}^{-1} \text{ s}^{-1}$) and a product distribution markedly affected by substituents. The hydroxyl radical is a strong electrophile and, in the case of aromatic rings, preferably adds at electron-rich sites [33]. For example, the attack of hydroxyl on aniline leads to *ortho*- and *para*-hydroxy compounds [34]. The stabilization of radical intermediates produced during the addition of hydroxyl radicals may take place by hydrogen abstraction or by electron transfer and proton elimination. Further reactions lead to ring opening and the formation of open conjugated structures.



Electron transfer is the other mechanism of hydroxyl oxidation, commonly encountered in oxidation of transition metal ions, which is also described in organic compounds in which large substituents avoid addition reaction [35].

2

Ozone Uses in Water Treatment

Ozone is used as the only oxidant or in association with other oxidants or energy (AOPs) in surface water, ground water or wastewater treatments. The ozone-based technologies have the common objective of optimizing the use of ozone to improve the disinfection or the removal of the pollutants present in water. The reason is not only the fact that it is an expensive oxidant, but also that it induces the generation of toxic oxidation intermediates. To reach this

goal, it is necessary to develop models whose level of complexity depends on the knowledge of the processes.

2.1

Precipitation of Oxides

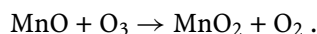
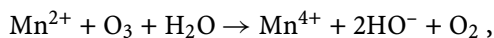
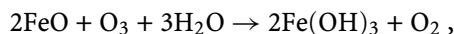
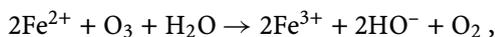
Iron and manganese are undesirable in drinking water because of their effect on the appearance and taste of the water, their ability to cause black or reddish staining or the formation of sediments. The rusty or brown stains on fabrics are of concern because they are not removed by usual detergents. Iron oxide deposits on tanks, water heaters and pipelines create problems of water supply related to equipment maintenance. These pollutants are not health threatening so the EPA does not set a mandatory water quality standard. The guideline standards for both these metals have been established in their soluble states, taking into account the growth of iron- and manganese-oxidizing bacteria that strongly affects the overall water quality.

In the United States, the National Secondary Drinking Water Regulations include secondary maximum contaminant levels (SMCLs) as a guideline to avoid aesthetic effects related to odour, taste and colour. Current SMCLs are 0.3 mg/L for iron and 0.05 mg/L for manganese. The Council Directive 98/83/EC on the quality of water intended for human consumption includes iron and manganese in Annex I, Part C, with values fixed only for monitoring purposes of 0.2 mg/L for iron and 0.05 mg/L for manganese.

The way iron and manganese should be removed depends on their oxidation state and concentration. Both can be present in water in dissolved form with oxidation states that depend on pH (Fe^{2+} , Mn^{2+} , Fe^{3+} , Mn^{4+}) or in colloidal particle suspension. Ground waters, being anaerobic, have higher iron and manganese contents than aerated water. In the latter case, the redox potential of the water allows the oxidation of reduced ionic forms into insoluble oxides. As concerns the oxidation mechanism, there is a certain controversy over whether it consists of an oxygen transfer from ozone to the reduced metal or an electron transfer from the reduced metal to ozone [36].

Iron and manganese are usually removed by oxidation of the dissolved forms into an insoluble form by aeration or by chemical oxidization followed by sand filtration. The success of removal by oxidation depends not only on the oxidant used and its concentration, but also on pH and on the presence of natural organic matter. Oxidation takes place at a faster rate at higher pH values and the presence of organic matter makes removal more difficult. Both iron and manganese tend to form bonds with humic acids and other natural organic matter compounds present in water. When air is used as oxidant this causes removal difficulties and in this case the oxidation with ozone is recommended. In general, the removal of iron is normally easier than that of manganese, but a high content of iron requires treatment with several tanks in series. It has been stated that the oxidation of iron with ozone is rapid,

but tends to form colloidal particles difficult to remove by sand or anthracite filtration [37]. The ozone dose required for oxidation can be estimated stoichiometrically as 0.43 mg/mg iron and 0.88 mg/mg manganese, the latter for $8.0 < \text{pH} < 8.5$, from the following reactions [38]:



Other oxidants may be used to remove iron and manganese by oxidation, but the dose of oxidant is higher. Table 2 shows the usual values for precipitation of iron and manganese from drinking water as a function of the oxidant [39].

The removal of oxides of iron and manganese may be carried out using different filtration media such as conventional beds of anthracite and sand with chemically bonded manganese oxide. The most suitable, however, is manganese greensand, a granular form of the zeolite mineral glauconite coated with manganese oxide that bonds due to the ion-exchange properties of glauconite [40]. This manganese-modified filtration medium also exhibits a catalytic effect in the chemical oxidation of iron and manganese removal. If necessary, the coating is regenerated by addition of potassium permanganate to oxidize the MnO to MnO₂. Backwashing of the greensand removes the precipitated oxides from the bed. A prefilter to remove most of the precipitated iron prior to the manganese greensand also prolongs the service run and reduces the pressure drop on the bed of greensand.

As concerns residual waters, ozone has been proposed to remove arsenic from the wastewater of nonferrous metallurgical industries [41]. Arsenic is a constituent of most sulphide ores and concentrates processed in nonferrous metallurgical industries. Process wastes have to be treated in an environmentally acceptable manner because of the environmental legal regulations. The National Primary Drinking Water Regulations (EPA) limit the levels of arsenic in drinking water to below 0.010 mg/L. Community water systems exceeding 0.005 mg/L (one half of the arsenic MCL) must notify their customers in their

Table 2 Commonly accepted dosing of oxidants required to remove iron and manganese from drinking water

| Oxidant | Iron (mg/mg Fe) | Manganese (mg/mg Mn) |
|------------------------|-----------------|----------------------|
| Chlorine | 0.62 | 1.27 |
| Chlorine dioxide | 1.21 | 2.45 |
| Potassium permanganate | 0.94 | 1.92 |
| Ozone | 0.43 | 0.88 |

annual reports. The Council Directive 98/83/EC also includes a maximum level of 0.010 mg/L (Annex I, Part B, Chemical Parameters).

The first step in the removal of arsenic takes place by precipitation by sulphide formation. The solubility of arsenic sulphide is about 30 mg/L, high enough to require a further treatment prior to discard to the environment. Ozone can be used to oxidize As(III) to As(IV), which in the presence of Mn(II) forms a precipitate with a Mn/As mole ratio around unity, believed to be $\text{MnAsO}_4 \cdot n\text{H}_2\text{O}$. The residual arsenic concentration depends on the initial manganese and iron concentrations and can be brought below the mandatory limit of 0.010 mg/L. The precipitation of arsenic with manganese by ozonation is also effective for removing arsenic in the pH range of 1–2 where ferric arsenate and ferric hydroxide do not precipitate. It has been reported that the conversion of As(III) to As(V) was fast with ozone with simultaneous oxidation of iron and manganese. The sequestering effect of the resultant As(V) played an important role. The sorption of freshly precipitated $\text{Fe}(\text{OH})_3$ was also significant and estimated to be 15.3 mg As/g $\text{Fe}(\text{OH})_3$ [42].

2.2

Disinfection of Drinking Water

Ozone has been used since 1919 in drinking water disinfection. It is a strong biocide which is able to deactivate resistant pathogen microorganisms resistant to chlorine and chlorine dioxide, such as *Cryptosporidium parvum* oocysts. The ozone-based technologies for drinking water disinfection try to provide operation conditions which do not favour indirect ozone reaction via hydroxyl radicals [43]. Ozone doses should eliminate and/or reduce the concentration of faecal microorganisms (faecal coliforms and *Escherichia coli*) to values that exclude any risk to human health. In case some pathogen microorganism refractory to ozone treatment exists, it is necessary to specifically determine the required ozone doses. With this object the *integral ct-exposure* parameter (*ct*) is defined by multiplying the disinfectant concentration in water by the time that the microorganism is in contact with it:

$$ct_{\text{O}_3} = \int C_{\text{O}_3} dt . \quad (20)$$

According to the microorganism deactivation model of Chick–Watson and assuming first-order deactivation kinetics, ct_{O_3} determines the reduction of viable microorganisms from an initial concentration N_0 to a final concentration N . For a given ozonation time in batch or plug flow:

$$\log \left(\frac{N}{N_0} \right) = -k_N \int_0^t C_{\text{O}_3} dt . \quad (21)$$

Equation 21 allows the calculation of the ozone necessary to obtain an efficient disinfection for a given microorganism with deactivation constant k_N [44]. The flow model permits the determination of the ozone concentration profile and therefore, the value of ct_{O_3} [45, 46]. When this information is not accessible, the usual solution is to multiply the concentration of ozone at the exit of the reactor by the time that 10% of an inert tracer injected by pulse is inside the reactor, ct_{10} .

The relationship between the concentration of ozone dissolved, C_{O_3} , and the total ozone dose (TOD) transferred can be obtained from Eq. 1, assuming first-order kinetics for ozone decomposition [47]:

$$C_{O_3} = \text{TOD} - X - k_d \int_0^t C_{O_3} dt, \quad (22)$$

$$\text{TOD} = \int_0^t k_L a (C_{O_3}^* - C_{O_3}) dt, \quad (23)$$

where X is the TOD at the beginning of the ozonation, where it is possible that the ozone decomposition is higher than the ozone absorption rate (mass transfer control) and the ozone dissolved is not detected. Solving Eq. 22 the following expression for X is obtained:

$$X = \text{TOD}_i = \int_0^t k_L a C_{O_3}^* dt. \quad (24)$$

From Eq. 22 and for a process in which flow follows the continuous stirred tank reactor (CSTR) model, the concentration of ozone inside the reactor is given by:

$$C_{O_3} = \frac{\text{TOD} - X}{1 + k_d \tau}, \quad (25)$$

where τ is the hydraulic retention time (HRT). From the Chick–Watson model and Eq. 25, the extent of the ozone disinfection in a CSTR, expressed as the relationship between the actual (N) and initial (N_0) concentration of microorganisms, is:

$$\frac{N}{N_0} = \frac{1}{1 + k_N \left(\frac{\text{TOD} - X}{1 + k_d \tau} \right) \tau}. \quad (26)$$

This equation connects the operational parameters TOD, X and τ and the kinetic parameters of the process (k_N , k_d , $k_L a$) with the required extent of disinfection. The deactivation constants for *E. coli*, *Bacillus subtilis* spores, *Rotavirus*, *Giardia lamblia* cysts, *Giardia muris* cysts and *Cryptosporidium*

parvum oocysts, which are refractory to ozonation, have been reported [43] but in general, data on microorganism deactivation kinetics are scarce.

2.3

Natural Water and Wastewater Treatment

The objectives of ozone-based treatments of surface water, ground water and wastewater are disinfection and the elimination of dissolved organic matter. Water dissolved organic compounds may present a huge variability in proportion and nature of pollutants (persistent organic pollutants (POPs), personal care products (PCPs), endocrine disruptors) depending on their source. The ozone-based technologies for natural water and wastewater treatment provide operation conditions favouring the direct or radical ozone reactions (AOPs). Ozone can be used as the only technology or in combination with other processes with the aim of improving coagulation–flocculation or biodegradability, to remove pollutants in natural water treatments or as a tertiary treatment in association with biological wastewater treatment [48].

Although the number of papers published on the efficiency of ozone to eliminate POPs and PCPs is considerable, the use of ozone is less extended in wastewater treatments than in disinfection or in natural water treatments [49–57]. Ozone is an expensive oxidant and the necessary doses in wastewater treatments are higher than in natural water, thus increasing operational costs. However, the ability of ozone to mineralize organic matter, alone or in association with other oxidants such as hydrogen peroxide, makes it especially attractive for new developments, in particular those for which the objective is the reuse of wastewater. The efficiency of the use of ozone requires new ozone generators as well as models of the ozonation process to optimize the ozone doses, thus reducing operational costs and avoiding toxic intermediates.

Figure 4 shows the evolution of total organic carbon (TOC) during the ozonation (O_3/H_2O_2 system) of aqueous solutions of a number of pollutants and their mixtures classified as PCPs: analgesics (dipyrone, diclophenac, acetyl salicylic acid), anti-inflammatories (ibuprofen), antiseptics (triclosan), antibiotics (tetracycline), antineoplastics (cyclophosphamide), anxiolytics (carbamazepine), hormones (oestradiol) and diagnostic compounds (acetamide). The ozonation processes were carried out in a semicontinuous mode in a 20-L bubble column reactor. Gas flowed at a rate of $0.36 \text{ Nm}^3 \text{ h}^{-1}$ ($k_L a = 5.6 \times 10^{-3} \text{ s}^{-1}$) with an ozone concentration of $29.7\text{--}40.3 \text{ g/Nm}^3$. The experiments were performed at pH values in the range 7.5–8.5, temperatures of $20\text{--}30 \text{ }^\circ\text{C}$ and a concentration of hydrogen peroxide of $1.0 \times 10^{-4} \text{ M}$. In all cases TOC_0 was reduced at least 50% during the first 30 min of ozonation. Table 3 shows representative results and operational conditions. With the aim of determining the nature of the final refractory organic carbon (TOC_c), the contribution of oxalate, acetate and formiate, the common ozonation end

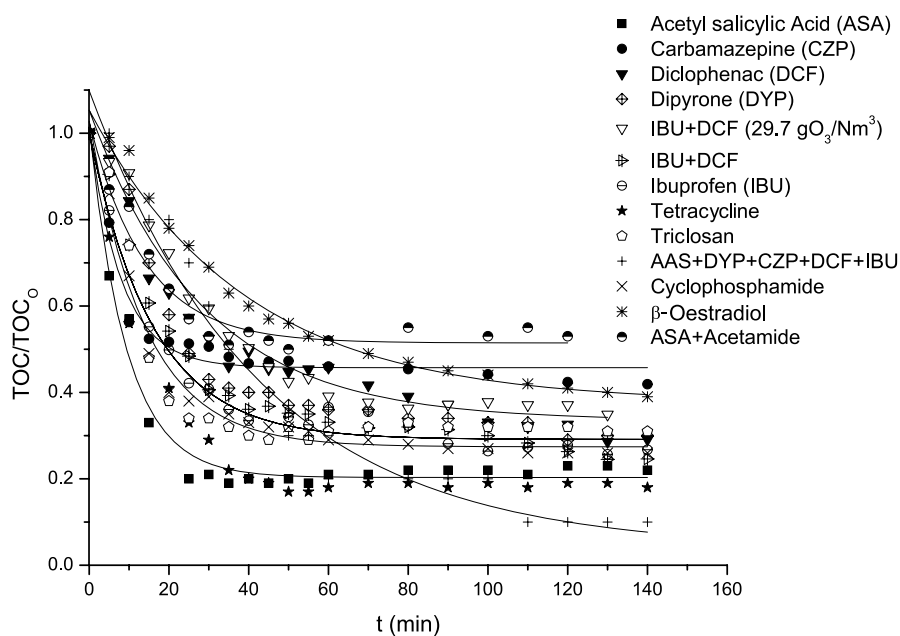


Fig. 4 Ozonation of PCPs in a 20-L bubble column reactor ($k_L a = 5.6 \times 10^{-3} \text{ s}^{-1}$). Experimental values of TOC versus time t for several compounds and mixtures. pH = 7.5–8.5, $T = 20\text{--}30^\circ\text{C}$, $[\text{H}_2\text{O}_2] = 1.0 \times 10^{-4} \text{ M}$; gas flow rate: $0.36 \text{ Nm}^3 \text{ h}^{-1}$, gas ozone concentration: $29.7\text{--}40.3 \text{ g/Nm}^3$

Table 3 Experimental data for the ozonation of PCPs and mixtures

| Compound | $\text{TOC}_0 \times 10^4$ (M) | O_3 (mM) | T ($^\circ\text{C}$) | pH | $(\text{TOC}_c / \text{TOC}_0)$ | $(\text{TOC}_c^* / \text{TOC}_0)$ | k (min^{-1}) |
|-------------------------|-----------------------------------|----------------------|-----------------------------|-----|---------------------------------|-----------------------------------|------------------------------|
| Acetyl salicylic acid | 9.7 | 0.84 | 24 | 7.8 | 0.21 | | 0.107 |
| Carbamazepine | 7.8 | 0.84 | 24 | 7.8 | 0.42 | 0.30 | 0.123 |
| Diclophenac | 6.7 | 0.84 | 24 | 7.6 | 0.29 | 0.22 | 0.037 |
| Dipyrone | 9.4 | 0.84 | 23 | 8 | 0.30 | 0.27 | 0.049 |
| IBU+DCF 10% pot | 14.5 | 0.62 | 24 | 7.8 | 0.35 | 0.17 | 0.035 |
| IBU+DCF 20% pot | 16.3 | 0.84 | 22 | 7.8 | 0.25 | 0.17 | 0.051 |
| Ibuprofen | 7.8 | 0.84 | 20 | 7.8 | 0.27 | 0.17 | 0.062 |
| Tetracycline | 7.7 | 0.84 | 23 | 7.8 | 0.18 | | 0.070 |
| Triclosan | 3.0 | 0.84 | 30 | 7.7 | 0.30 | | 0.083 |
| ASA+DYP+CZP+ IBU+DCF | 32.4 | 0.84 | 22 | 7.8 | 0.15 | | 0.023 |
| Cyclophosphamide | 8.8 | 0.84 | 24 | 7.8 | 0.26 | | 0.071 |
| β -Oestradiol | 2.0 | 0.84 | 24 | 7.8 | 0.39 | | 0.026 |
| ASA+acetamide | 17.3 | 0.84 | 24 | 7.8 | 0.53 | 0.40 | 0.071 |

products, were measured (TOC_c^* in Table 3). The experimental data of TOC were fitted with pseudo first-order kinetic expressions like Eq. 25 and kinetic constants are shown in Table 3:

$$\ln \frac{\text{TOC}}{\text{TOC}_0} = kt. \quad (27)$$

As in disinfection of drinking water, the ozonation models for wastewater must relate process conditions and kinetic parameters with the ozone dose required to remove pollutants. The supply of ozone is determined from a selected parameter whose value must be reduced. Depending on the information available about the wastewater, the object will be the reduction of one of various specific pollutants or to lower global parameters such as TOC or chemical oxygen demand (COD). The basic knowledge about the ozonation process determines how close the model is to reality. It is possible that in wastewater from a given industrial process the ozonation kinetic constants of the main pollutants can be available. In most cases the reaction paths of compounds present in wastewater matrices and their elimination kinetic constants are not known and therefore a global approach is normally preferred.

In the experiment of Fig. 2, where ozonation by a radical pathway is not favoured, an elimination of TOC close to 10% was observed during the first 4 min of reaction (zone I). The ozone decomposition kinetic constant was $k_d = 0.139 \text{ min}^{-1}$ obtained by solving Eq. 28 as in Sect. 1.3:

$$\frac{dC_{O_3}}{dt} = -k_d C_{O_3}. \quad (28)$$

The TOC removal kinetic constant was $k = 0.78 \text{ min}^{-1}$, obtained by fitting the experimental TOC values of Fig. 2 with a pseudo first-order kinetic equation. Although this approach can characterize the kinetics of the process, it does not relate the ozone dissolved concentration with TOC in order to calculate the ozone dosing. Taking into account that the elimination of pollutants in water by ozone is due to direct and indirect (radical) reactions, Elovitz and von Gunten [24] proposed a model for the removal of specific micropollutants in which the ozonation process is characterized by a parameter R_{ct} defined as the relationship between the integral ct -exposure to ozone and the hydroxyl radical, the two principal oxidants in the system:

$$R_{ct} = \frac{\int C_{HO\cdot} dt}{\int C_{O_3} dt} \quad (29)$$

The R_{ct} parameter characterizes the ozonation process and allows estimation of the concentration of the hydroxyl radical in water from the concentration of dissolved ozone. The balance of a determined pollutant (P) with C_{P_0} initial concentration in water in a volume element of the reactor either in *batch* or *plug flow* during an ozonation process follows the expression of Eq. 30.

The kinetic constants k_{O_3} and k_{HO^\cdot} are linked with direct and indirect ozone reactions, respectively. R_{ct} connects the extent of decontamination with the integral ct -exposure of ozone:

$$\ln \frac{C_P}{C_{P_0}} = k_{O_3} \int_0^t C_{O_3} dt + k_{HO^\cdot} \int_0^t C_{HO^\cdot} dt = (k_{O_3} + R_{ct}k_{HO^\cdot}) \int_0^t C_{O_3} dt \quad (30)$$

From Eqs. 30 and 22 the ozone requirements (concentration of ozone in water and TOD) can be linked with the elimination level of pollutants. The low concentration values of the hydroxyl radical in water ($C_{HO^\cdot} \leq 10^{-12}$ M) make its direct measurement practically impossible. However, the integral $\int C_{HO^\cdot} dt$ may be determined by means of probe compounds [58, 59], such as *p*-chlorobenzoic acid (*p*CBA), whose direct and indirect kinetic constants are known ($k_{O_3/pCBA} \approx 0.15 \text{ M}^{-1} \text{ s}^{-1}$, $k_{HO^\cdot/pCBA} \approx 5 \times 10^9 \text{ M}^{-1} \text{ s}^{-1}$). A balance to *p*CBA leads to the following expression to the integral ct -exposure to HO^\cdot :

$$\frac{\ln \frac{pCBA}{pCBA_0}}{k_{HO^\cdot}} = \int C_{HO^\cdot} dt. \quad (31)$$

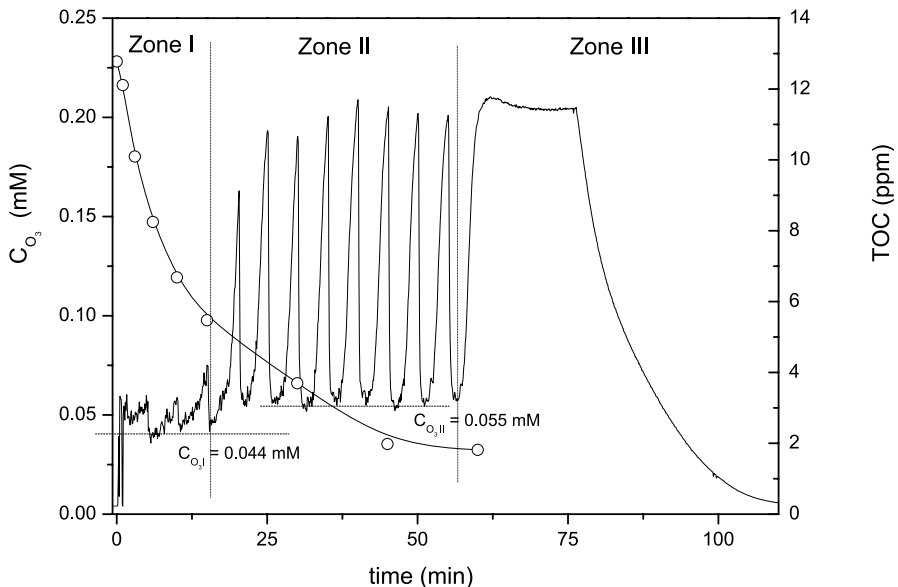


Fig. 5 Evolution of TOC (○) and ozone concentration during treatment of D070208 wastewater (Table 4) with O_3/H_2O_2 . pH = 8.04–8.25, $T = 25^\circ\text{C}$; gas flow rate: $0.36 \text{ Nm}^3 \text{ h}^{-1}$, gas ozone concentration: 45.9 g/Nm^3 ; $k_{La} = 0.614 \text{ min}^{-1}$ and injection of 0.15 mL of H_2O_2 (30% w/v) every 5 min

Table 4 Reaction conditions and kinetic parameters of the ozonation (O_3/H_2O_2) of domestic (D) and urban (U) wastewater at $T = 25^\circ C$, $pH = 7.6-8.2$ and $K_L a = 0.614 \text{ min}^{-1}$ (f: sample filtered before ozonation)

| Sample | TOC ₀ (ppm) | TOC removed (%) | C _{O₃gas} (mM) | C _{O₃*} (mM) | C _{O₃I} (mM) | k _{dI} (min ⁻¹) | R _I (mM ⁻¹ min ⁻¹) | C _{O₃II} (mM) | k _{dII} (min ⁻¹) | R _{II} (mM ⁻¹ min ⁻¹) | C _{O₃III} (mM) | k _{dIII} (min ⁻¹) |
|----------------------|---------------------------|-----------------------|---------------------------------------|-------------------------------------|-------------------------------------|---|---|--------------------------------------|--|--|---------------------------------------|---|
| D070206 ^f | 15.51 | 91.3 | 1.010 | 0.233 | 0.038 | 3.26 | 0.823 | 0.050 | 2.32 | 0.125 | 0.198 | 0.112 |
| D070208 ^f | 12.77 | 85.8 | 1.039 | 0.240 | 0.075 | 1.36 | 1.084 | 0.091 | 1.01 | 0.375 | 0.204 | 0.109 |
| D070308 | 12.17 | 62.7 | 1.021 | 0.236 | 0.120 | 0.42 | 0.996 | 0.134 | 0.33 | 0.084 | 0.190 | 0.104 |
| D070417 | 8.45 | 85.4 | 1.019 | 0.235 | 0.049 | 1.51 | 0.337 | 0.070 | 0.94 | 0.192 | 0.199 | 0.072 |
| D070419 | 14.04 | 76.4 | 1.021 | 0.236 | 0.050 | 2.25 | 0.496 | 0.078 | 1.22 | 0.047 | 0.206 | 0.088 |
| U070205 ^f | 11.89 | 90.5 | 1.000 | 0.231 | 0.027 | 3.20 | 1.226 | 0.043 | 1.85 | - | 0.202 | 0.061 |
| U070208 ^f | 8.98 | 100 | 1.035 | 0.239 | 0.037 | 3.20 | 2.130 | 0.056 | 1.91 | - | 0.202 | 0.107 |
| U070222 | 8.56 | 92.1 | 1.039 | 0.240 | 0.053 | 2.20 | 1.744 | 0.090 | 1.04 | 0.261 | 0.209 | 0.093 |
| U070305 | 11.85 | 88.4 | 1.071 | 0.247 | 0.054 | 2.25 | 0.513 | 0.067 | 1.69 | - | 0.210 | 0.111 |
| U070308 | 15.54 | 85.6 | 1.034 | 0.239 | 0.038 | 2.04 | 0.220 | 0.051 | 1.42 | 0.165 | 0.188 | 0.105 |
| U070416 | 8.76 | 94.2 | 1.035 | 0.239 | 0.043 | 2.77 | 1.270 | 0.065 | 1.63 | 0.159 | 0.201 | 0.115 |
| U070419 | 8.38 | 95.0 | 1.031 | 0.238 | 0.051 | 2.48 | 0.525 | 0.068 | 1.69 | - | 0.205 | 0.109 |

Table 5 Characterization of domestic (D) and urban (U) wastewaters

| Sample | Suspended solids (mg/L) | Conductivity (μS) | pH | COD (mg L^{-1}) | Alkalinity (ppm CaCO_3) | NO_3^- (ppm) | PO_4^{3-} (ppm) | SO_4^{2-} (ppm) | Cl^- (ppm) | NH_4^+ (ppm) |
|---------|-------------------------|--------------------------------|------|----------------------------|-----------------------------------|-----------------------|--------------------------|--------------------------|---------------------|-----------------------|
| D070206 | 12.8 | - | 7.98 | 44 | 528.14 | 2.56 | 9.64 | 111.46 | 59.80 | 41.27 |
| D070208 | 12.8 | - | 8.04 | 44 | 495.52 | 2.12 | 7.97 | 112.42 | 62.24 | - |
| D070308 | 10.1 | 368 | 7.76 | 182 | 419.37 | 2.12 | 5.16 | 84.93 | 51.84 | 36.04 |
| D070417 | 0.55 | 631 | 8.12 | 81 | 579.93 | 3.01 | 12.91 | 86.39 | 54.59 | 49.76 |
| D070419 | 7.45 | 579 | 8.38 | 66 | 521.38 | 5.43 | 11.61 | 80.69 | 54.54 | 42.56 |
| U070205 | 3.6 | - | 8.01 | 42 | 539.23 | 14.69 | 8.18 | 126.5 | 77.49 | - |
| U070208 | 12.4 | - | 8.11 | 35 | 507.67 | 12.45 | 13.03 | 131.59 | 75.78 | - |
| U070222 | - | 407 | 7.61 | 62 | 454.57 | 11.57 | 7.09 | 102.83 | 67.84 | 28.32 |
| U070305 | 11.6 | 492 | 7.66 | 71 | 497.44 | 14.46 | 6.39 | 114.26 | 73.64 | 30.25 |
| U070308 | 0.65 | 446 | 7.59 | 54 | 415.29 | 47.82 | 4.87 | 90.60 | 61.36 | 16.05 |
| U070416 | - | 601 | 7.65 | 67 | 475.17 | 95.83 | 2.53 | 116.25 | 78.47 | 1.14 |
| U070419 | - | 548 | 7.94 | 52 | 344.64 | 30.52 | 1.34 | 101.46 | 81.35 | 9.39 |

Figure 5 shows the evolution of ozone and TOC during the ozonation of the same wastewater of Sect. 2.3 (D070208, Table 5). Reaction conditions were the same as in Sect. 2.3 but equal volumes (0.15 mL) of hydrogen peroxide (30% w/v) were injected every 5 min in order to favour the TOC elimination by a radical pathway. Three zones that correspond with three different ozone decomposition and TOC elimination kinetics can be observed. The TOC that remained in zone III is refractory to ozonation. In zone III injections of hydrogen peroxide were stopped to avoid ozone decomposition by that compound, thereby allowing the concentration of ozone to reach a stationary state ($C_{O_3} = 0.204$ mM). In the later part of zone III, the concentration of ozone decreased once gas flow was stopped. The conditions in zone III allow the determination of $k_{dIII} = 0.109$ min⁻¹ and $k_{La} = 0.619$ min⁻¹. In zones I and II the ozone fluctuations are due to the decomposition induced by hydrogen peroxide. In these two zones two minimums $C_{O_3I} = 0.075$ mM and $C_{O_3II} = 0.091$ nM may be identified as indicated in Fig. 5. Assuming that these two values could correspond with two stationary states of the process, the ozone decomposition kinetic constants for each zone can be calculated: $k_{dI} = 1.36$ min⁻¹ and $k_{dII} = 1.01$ min⁻¹.

Assuming that, due to reaction conditions, the ozonation proceeds by a radical mechanism, Eq. 30 applied to TOC leads to the following expression:

$$\ln \frac{TOC_0}{TOC} = R_{ct} k_{HO} \cdot \int C_{O_3} dt = R \int C_{O_3} dt. \quad (32)$$

Figure 6 shows the logarithmic plot of TOC removal as a function of the integral ozone exposure following Eq. 32. Two different TOC removal zones, identified with zones I and II in Fig. 5, can be observed. The corresponding slopes are $R_I = 1.084$ mM⁻¹ s⁻¹ and $R_{II} = 0.375$ mM⁻¹ s⁻¹.

The parameter R allows a kinetic characterization of the ozonation processes even though global parameters to measure the contamination in water such as TOC or COD are used. As said before, from Eqs. 32 and 22 the ozone requirements for a given degree of TOC removal can be linked. Table 4 shows the TOC removed and the experimental values of R , k_d and ozone concentration at the different steps of ozonation of two kinds of wastewaters: domestic (D) and urban (U) from the secondary clarifier of two municipal wastewater treatment plants. Wastewaters were treated by ozonation processes with the O_3/H_2O_2 system as indicated before. With the aim of reflecting the seasonal variability of wastewater, the samples were collected at different dates. The main characteristics of the wastewater are shown in Table 5.

Yurteri and Gurol [60] related the ozone decomposition kinetic constant k_d with pH, alkalinity (Alk) and TOC. These researchers found a deviation within $\pm 25\%$ between k_d estimated by the empirical Eq. 33 and the experimental values determined by Eq. 34 in ozonation processes of surface water

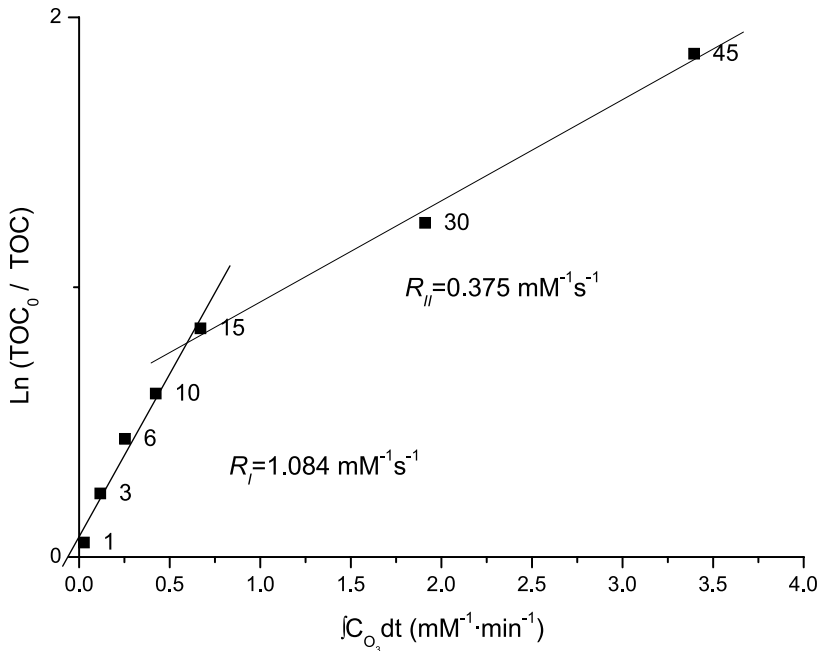


Fig. 6 Determination of kinetic parameters R for the ozonation. Treatment of D070208 wastewater (Table 4) with O_3/H_2O_2 . pH = 8.04–8.25, $T = 25^\circ C$; gas flow rate: $0.36 \text{ Nm}^3 \text{ h}^{-1}$, gas ozone concentration: 45.9 g/Nm^3 ; $k_{La} = 0.619 \text{ min}^{-1}$ and injection of 0.15 mL of H_2O_2 (30% w/v) every 5 min

and wastewater (pH = 6.8–9.0, TOC = 0.3–5.3, Alk = 10–500 mg/L $CaCO_3$).

$$\log k_d = -3.98 + 0.66\text{pH} + 0.61 \log \text{TOC} - 0.42 \log (\text{Alk}/10) \quad (33)$$

$$-\frac{dC_{O_3}}{dt} = k_d C_{O_3} \quad (34)$$

The removal of specific pollutants during an ozonation process can be performed by considering separately the direct reaction with ozone and the radical chain propagation with hydroxyl radical:

$$\frac{dC_M}{dt} = -(zk_D C_{O_3} + k_{HO\cdot} C_{HO\cdot}) C_M \quad (35)$$

The corresponding balance to ozone may take into account the initiation and termination reactions as well as reaction with the organic intermediates:

$$\begin{aligned} \frac{dC_{O_3}}{dt} = & k_{La}(C_{O_3}^* - C_{O_3}) - (k_{HO\cdot} C_{HO\cdot} + k_{HO_2\cdot} C_{HO_2\cdot}) C_{O_3} \\ & - (k_D C_M + \sum k_{Di} C_{Mi}) C_{O_3} - \sum k_{r} C_r C_{O_3} \end{aligned} \quad (36)$$

The usefulness of these models to determine the requirement of ozone depends on knowledge about (1) the stoichiometry of the direct ozone reaction, (2) the direct kinetic constants of ozone with M and with reaction products M_i , (3) the kinetic constant of hydroxyl reaction with M and (4) the ozone decomposition kinetic constants due to other radical species in water, k_r . Glaze and Kang [61,62] and Beltran et al. [63] solved a similar set of equations to determine the removal of low molecular weight halogenated compounds, polynuclear aromatics and nitroaromatic hydrocarbons. The concentration of radical species in solution was determined in all cases by assuming a stationary state.

2.4

Catalytic Ozonation

The homogeneous rate of production of hydroxyl radicals from ozone is strongly dependent on pH, since the active species in the initiation of the ozone decomposition mechanism are HO^- and HO_2^- , the concentrations of which are directly related to the concentration of hydroxide [15, 16]. However, the ozonation under alkaline conditions presents an important drawback in the case of water with bromine levels higher than $50 \mu\text{g/L}$ due to the formation of bromate as oxidation by-product [43]. Excessive bromate formation is a major concern due to its potential carcinogenicity, which imposed a limit of $10 \mu\text{g/L}$ in drinking water standards both in the United States and Europe. Besides limiting ozone exposure, a recommended strategy to reduce bromate formation is to use $\text{pH} < 7$ because bromate formation is also strongly pH dependent [64]. On the other hand, under acidic conditions the formation of hydroxyl radicals and the rate of mineralization are much lower than in conventional ozonation. In this situation, a catalyst may be used to promote ozone decomposition, ozonation reactions or both. Other advanced technologies for water and wastewater treatment currently under development may avoid bromate formation. Sonochemical methods, photolysis or photocatalysis, Fenton processes or certain combinations with conventional technologies like adsorption, wet oxidation, membrane separations or biological treatment might compete with ozonation. To date, however, only ozone-based technologies have been widely used in water treatment plants, which justifies the effort to develop catalytic processes able to operate in acidic media.

Another important drawback of conventional homogeneous ozonation that might be overcome by using a catalyst is the inhibition due to the presence of carbonates, bicarbonates and other radical scavengers. The case of carbonates and bicarbonates is especially obvious not only from their presence in natural water and wastewater, but also because they are products of the mineralization reactions. Inhibitors reduce the efficiency of an ozonation process and cause a poor mineralization due to the persistency of intermediate oxidation products. Short-chain carboxylic acids represent a class of

organic compounds particularly refractory to the oxidation by ozone. Acids such as pyruvic, glyoxalic or oxalic are normally produced during the ozonation of complex organic molecules, their refractory character being responsible for most of the organic content of treated wastewaters. A number of attempts have been made to remove these compounds during ozonation using catalysts in either the homogeneous or heterogeneous phase [65–69]. An important question about the behaviour of carboxylic acids in a heterogeneous catalytic system is the ability of the catalyst to adsorb the organic substrate. This point will be discussed below.

It has been suggested that the combination of ozonation and adsorption on activated carbon in a single process is an alternative to the treatment of wastewaters containing organic contaminants [70]. As revealed before, the ozonation efficiency for carbon removal is limited due to the formation of refractory short-chain carboxylic acids. On the other hand, activated carbon becomes saturated easily when treating wastewaters with high organic content, requiring frequent regeneration or replacement [71]. The ozonation on activated carbon may allow these limitations to be overcome because of a high adsorption capacity combined with high surface area and catalytic activity due surface metals and other surface chemical properties. The catalytic mechanism of ozonation on activated carbon is still unclear, but most results suggest that the role played by carbon is essentially to promote the decomposition of ozone with a subsequent increase in the production of radicals. The hydroxyl radicals formed would not be bonded to the surface, being free to react in the aqueous phase. Therefore, activated carbon would behave as an initiator of the radical-type chain reaction that transforms ozone into hydroxyl radicals.

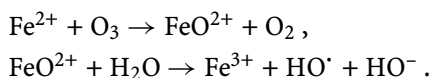
In what follows, attention will be focused on homogeneous catalytic systems and the ozonation on metals and metal oxides. By far the most commonly tested catalysts for the ozonation of organic compounds are supported and unsupported metals and metal oxides, especially titanium oxide and manganese oxide [66, 67, 72]. There is a certain controversy on the mechanism of ozonation on ionizable surfaces. Some authors assume the formation of surface oxidation sites able to interact with organic compounds [73]. Ma and Graham [74] suggested a mechanism based on the initiation of ozone decomposition by hydroxide ions linked to the negatively charged surface of manganese oxide. The interaction of organic solutes with charged surfaces must be relevant and will be discussed below. Ozonation on supported metals has been less studied. Lin et al. [19, 75] reported a considerable efficiency for the removal of formic acid on Pd and Pt on alumina. Noble metals, especially when supported on SiO₂, also showed appreciable activity for the decomposition of ozone in water and are candidates to catalyse an ozonation process. The ozonation of carboxylic and chlorinated carboxylic acids on Ru/CeO₂ and Ru/CeO₂-TiO₂ have been reported by Karpel et al. [76] and Fu et al. [77]. The results of ozonation on metals and metal oxides have in common a strong de-

pendence of the reaction rate on the mode of preparation of the catalyst and on support pre-treatment. These variables should affect the interaction of the molecule with the surface and its adsorption capability for ozone or organic molecules.

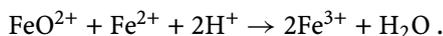
2.4.1 Homogeneous Catalytic Ozonation

Earlier works showed that certain metals in solution are able to increase the removal of organics from aqueous solution with respect to non-catalytic ozonation [78]. The catalytic activity of Fe(II), Fe(III), Mn(II), Ni(II), Cr(III), Ag(I), Cu(II), Co(II), Zn(II) and Cd(II) have been reported [79].

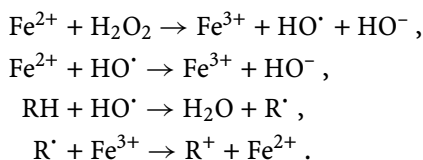
It has been proposed that the mechanism of homogeneous ozone-metal systems is based on the generation of hydroxyl radicals through an ozone decomposition reaction [80]:



On the other hand, Novell and Hoigné [81] indicated that the production of hydroxyl radicals cannot be directly related to the interaction of ozone with the transition metal and the latter reaction should be substituted by the following one:

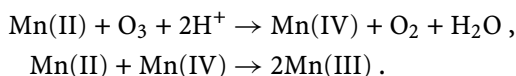


In addition to this, the iron-catalysed ozonation may share reactions with the classical Fenton homogeneous process. The interaction of ozone and water is known to produce hydrogen peroxide, which may produce hydroxyl radicals:

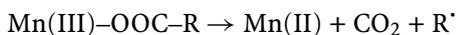
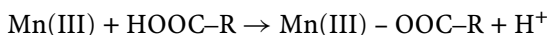


Organic radicals should play an important role in the reduction of Fe(III), but the regeneration of the catalyst may take place by other mechanisms with the intervention of hydroperoxy radicals, HO_2^\cdot [82].

Oxalic acid tends to form complexes with transition metals such as manganese, iron and cobalt. The formation of these complexes plays an important role in the catalytic mechanism of ozonation [83]. Andreozzi et al. [66] studied the ozonation of glyoxalic acid catalysed by manganese salts and suggested a mechanism of oxidation mediated by Mn(III):



Mn(III) reacts with an acid moiety originating the abstraction of CO₂ with the consequent reduction of Mn(III) to Mn(II).

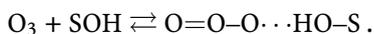
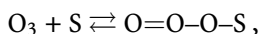
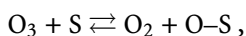


The formation of complexes has also been proposed for the ozonation of oxalic acid using Co(II) by Pines and Reckhow [83]. In this case the Co(II) complex is oxidized by ozone to a Co(III) form with subsequent elimination of Co(II), resulting in an oxalate radical anion which further decomposes.

2.4.2

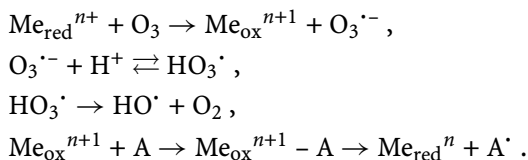
Catalysis by Metals and Metal Oxides

The mechanism of catalytic ozonation on oxides and metals may involve the adsorption of ozone, but not necessarily the adsorption of organic pollutants. It has been demonstrated that dissolved ozone adsorbs and decomposes on many solid surfaces other than activated carbon, the resulting radicals being responsible for indirect oxidation reactions [25, 75]. This mechanism relies on the well-known result that gas-phase ozone adsorbs on solid surfaces to yield different molecular or ionic species. Dhandapani and Oyama [84] reported that ozone decomposition on p-type oxides is consistent with the formation of superoxide (O₂⁻) or peroxide (O₂²⁻) species on the surface. Bullanin et al. [85] suggested that on the stronger Lewis sites ozone dissociates after adsorption to yield a surface oxygen atom. With weaker sites, ozone molecules form a coordination bond via one of the terminal oxygen atoms. Another possibility is the formation of weak hydrogen bonds with surface OH groups:

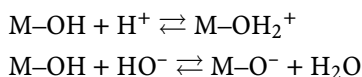


In the case of metals and metal oxides, the catalytic reaction may also involve the adsorption of organic molecules or ions on surface sites leading to two additional mechanisms. The first possibility is an Eley-Rideal interaction between an adsorbed organic molecule and ozone or radicals from the bulk aqueous phase. On the other hand, an adsorbed organic molecule can react with adsorbed ozone or the products of surface ozone decomposition. Legube and Karpel [36] proposed a redox version of the latter for heterogeneous ozonation on metals, in which the ozone oxidizes surface metal atoms with the generation of hydroxyl radicals. Organic molecules are oxidized by electron transfer from the catalyst yielding back the reduced form of the metal

and organic radical species:



The adsorption of neutral organic compounds on Lewis acid sites is difficult due to the competitive adsorption of water molecules on the surface. Moreover, at basic pH, the hydroxide anion should prevent any adsorption on Lewis sites. Surface interaction is easier for ionizable organic molecules in aqueous solution if the surface is charged and allows ion exchange. The surface of metal oxides exhibits ion-exchange properties and the hydroxyl groups formed behave as Brönsted acid sites and dissociate depending on the pH of the solution.



If K_1 and K_2 are the ionization constants for the preceding surface equilibria, the point of zero charge (PZC) represents the pH at which the surface is not charged:

$$\text{pH}_{\text{PZC}} = \frac{pK_1 + pK_2}{2}. \quad (37)$$

A neutral organic compound may adsorb on metal oxide surfaces provided it is a strong enough Lewis base and the pH of the solution is near pH_{PZC} of the oxide. Otherwise, it is reasonable to assume that only ionizable substances would be capable of interacting with charged surfaces. Carboxylates, for example, adsorb on positively charged surfaces by exchanging the corresponding counteranion [18].

The kinetics of adsorption may play an important role in the ozonation process. Figure 7 shows some results for the adsorption of naproxen ($\text{p}K_a = 4.60$) and carbamazepine ($\text{p}K_a = 14.0$) on TiO_2 Degussa P25 with pH_{PZC} of 6.8 [86] and $\text{TiO}_2/\text{Al}_2\text{O}_3$ with pH_{PZC} of 8.3, prepared by impregnation with titanium isopropoxide following the method of Zhaobin et al. [87]. As expected from the PZC of the surface, adsorption is favoured for naproxen under acidic conditions at which the surface behaves as an anion exchanger [88]. Carbamazepine does not dissociate in acidic solutions and consequently its adsorption pattern is similar for pH values in the range 3–7. Similar results have been published for other acidic solutes [67, 89]. The results indicate that the rate of adsorption may be slow enough to control the overall kinetics. For the drugs mentioned above, the adsorption ranged only 5–15% from their equilibrium value during the first hour. Even for naproxen at $\text{pH} = 3$, below its $\text{p}K_a$ the adsorption was slow and equilibrium required a day or more in most

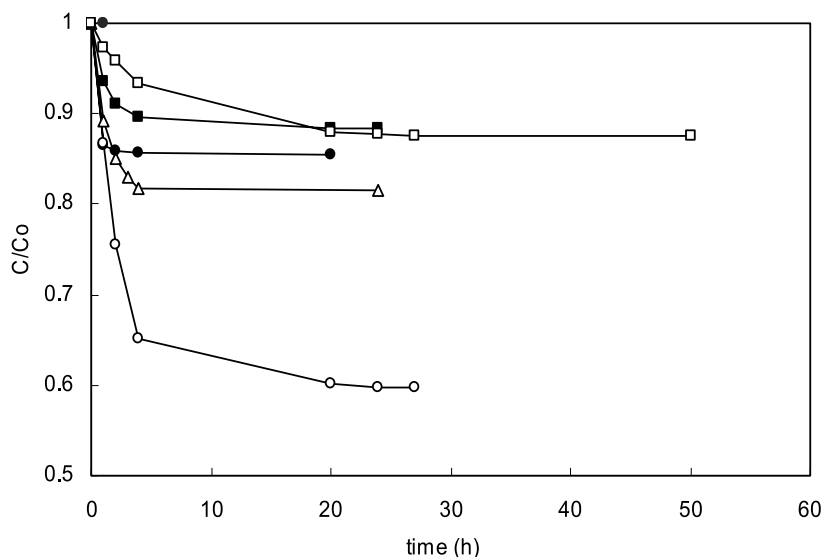
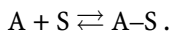


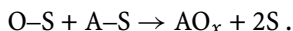
Fig. 7 Dimensionless concentration of naproxen during adsorption on TiO₂/Al₂O₃ at pH = 5 (□), on TiO₂ P25 at pH = 3 (○), on TiO₂ P25 at pH = 7 (■) and carbamazepine on TiO₂ P25 at pH = 5 (●) and pH = 7 (△). Temperature 25 °C, catalyst loading 1 g/L, initial concentration 6.0–6.5 × 10⁻⁵ M

cases. This agrees with several pieces of data showing that the adsorption of acid pollutants on metal catalysts supported on alumina is slow, taking from hours to days to complete [68, 89]. A kinetic model of ozonation should take into account this possibility.

Without explicit consideration of the surface charge, the ozonation mechanisms that involve the adsorption or ion exchange of an organic compound start with the bonding of the adsorbate to a vacant site (S). The adsorbate (A) would displace coordination water and bond to the surface:



The reaction may then take place between adsorbed organic solute and an oxidized site on the catalytic surface following a Langmuir–Hinshelwood mechanism:



Alternatively, dissolved ozone or hydroxyl radicals in solution may react with the adsorbed organic compound through an Eley–Rideal interaction:



Some organic compounds react with dissolved ozone at a high rate. This is the case for drugs such as naproxen and carbamazepine mentioned above. Anyway, the mineralization rate is slow in non-catalytic systems in acidic

conditions, so that the design of catalytic reactors is focused on refractory compounds under conditions in which direct reactions can be ignored. The rate of reaction of an organic compound combines the homogeneous reaction with hydroxyl radicals and the heterogeneous reaction of hydroxyl (or ozone) with solute with at least one reagent adsorbed.

If the reaction takes place between adsorbed species and hydroxyl radicals from the bulk, the Eley-Rideal rate expression would be as follows:

$$-\frac{dC_A}{dt} = k_{HO} \cdot C_{HO} \cdot C_A + k_c C_s C_{HO} \cdot \theta, \quad (38)$$

where θ is the fraction of surface sites occupied by adsorbate and C_s the bulk concentration of solids. Accepting the R_{ct} concept of Elovitz and von Gunten [24], the ratio of hydroxyl radicals and ozone at any time is constant over a wide range of the ozonation process:

$$R_{ct} = \frac{C_{HO}}{C_{O_3}}. \quad (39)$$

If the catalytic reaction with the adsorbed organic compound is the rate-limiting process, an adsorption equilibrium exists at any time. Using k_a and k_d to denote the adsorption and desorption kinetic constants, Eq. 38 can be rewritten as follows:

$$-\frac{dC_A}{dt} = k_{HO} \cdot R_{ct} C_{O_3} C_A + k_c C_s R_{ct} C_{O_3} \frac{k_a C_A}{k_a C_A + k_{-a}}. \quad (40)$$

If surface coverage is low, Eq. 40 can be simplified by assuming that $k_a C_A \ll k_{-a}$:

$$-\frac{dC_A}{dt} = (k_{HO} \cdot R_{ct} + k_c C_s R_{ct} K_a) C_{O_3} C_A. \quad (41)$$

The adsorption equilibrium constant, K_a , becomes included in a group of constants with a linear dependence on catalyst load. Equation 41 can be integrated to obtain explicitly the time-integrated concentration of ozone:

$$\ln \frac{C_{A,o}}{C_A} = (k_{HO} \cdot R_{ct} + k_c C_s R_{ct} K_a) \int C_{O_3} dt. \quad (42)$$

A similar result would be obtained for a reaction between adsorbed organic compounds and oxidized catalyst sites, provided that the elementary surface step is rate controlling and an adsorption equilibrium exists at any time for both reagents:

$$-\frac{dC_A}{dt} = k_{HO} \cdot R_{ct} C_{O_3} C_A + \frac{k_c C_s C_{O_3} C_A}{(1 + K_a C_s) (1 + K_{ox} C_{O_3})}, \quad (43)$$

where K_{ox} represents the equilibrium constant of the surface oxidation step. If the equilibrium constants are small, the surface step would be first order in

the oxidant and in the organic compound and the differential and integrated rate equation would be similar to Eqs. 41 and 42, respectively.

A surface redox mechanism such as that involved in ozonation has sometimes been described by means of a Mars–van Krevelen rate expression. The rate of catalytic reaction would depend on the rate of the oxidation process, k_o , and the rate of the organic compound with the oxidized catalyst, k_c . Assuming that the ozone is the oxidant and ignoring the surface stoichiometric coefficient, the rate of organic depletion would be as follows:

$$-\frac{dC_A}{dt} = k_{HO} \cdot R_{ct} C_{O_3} C_A + \frac{k_o k_c C_s C_{O_3} C_A}{k_o C_{O_3} + k_c C_A} \quad (44)$$

If the rate of catalyst oxidation is low, the catalytic reaction would be zero order in the organic compound. Conversely, for a high rate of surface oxidation, the reaction rate would be independent of the concentration of oxidant and first order in the oxidized organic compound. The resulting equations can be integrated and yielded equations somewhat different from Eq. 42. Although relatively common in catalysis, the Mars–van Krevelen approach recently received some criticism concerning its fundamental background. Vannice [90] proved that the kinetic expression is incorrect and that the obtained reaction orders can be derived from the Langmuir–Hinshelwood equation under more transparent assumptions.

On the other hand, if adsorption of organics is so slow that it controls the overall kinetics, the rate of the catalytic process would be independent of the concentration of ozone or other oxidants:

$$-\frac{dC_A}{dt} = k_{HO} \cdot R_{ct} C_{O_3} C_A + k_a C_s C_A \quad (45)$$

The integration of Eq. 45 leads to an expression in which the logarithmic decrease of the organic compound is not linear in the time-integrated concentration of ozone:

$$\ln \frac{C_{A,o}}{C_A} = k_{HO} \cdot R_{ct} \int C_{O_3} dt + k_a c_s t \quad (46)$$

The mechanisms described in Eqs. 42 and 46 can be discriminated by using kinetic data. For example, Eq. 42 predicts that a change in the concentration of ozone should have no effect in the logarithmic decrease of the concentration of a given compound, while Eq. 46 suggests that decreasing the ozone dose would lead to a time-integrated concentration in more time and, therefore, to a greater conversion of the organic compound.

If an aggregate such as TOC is used instead of the concentration of a single compound, the kinetic expressions would show the evolution of mineralization with the time-integrated concentration of ozone. Figure 8 shows experimental data corresponding to the ozonation of naproxen (6.5×10^{-5} M in pure water) using titanium dioxide Degussa P25 as catalyst and in non-catalytic runs performed in the same conditions. Ozone was continuously

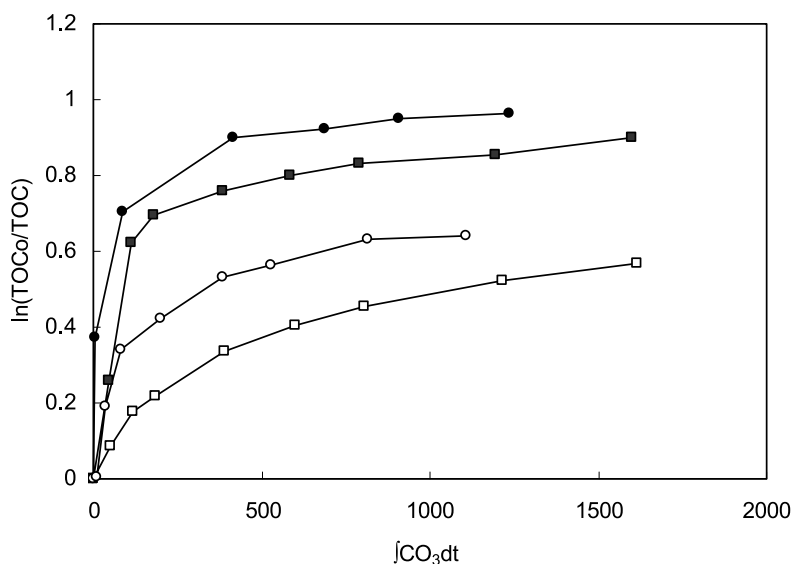


Fig. 8 Mineralization during the ozonation of naproxen (6.5×10^{-5} M) on TiO₂ P25 at pH = 3 (■) and pH = 5 (●) at 25 °C and catalyst loading of 1 g/L. Empty symbols correspond to non-catalytic runs under the same conditions. The units of the integral ozone exposure are mM s

bubbled from a corona discharge ozone generator and the steady-state concentration of ozone in the liquid was 0.230 mM.

Data show the existence of two different mineralization periods. During the first period most of the TOC decay takes place, the reaction being considerably accelerated by the presence of catalyst. The second period was essentially independent of pH and reflects the slow mineralization of refractory compounds. The similitude between catalytic and non-catalytic plots hides at least one fundamental difference between both processes. Figure 9 shows the concentration of oxalate measured by ion chromatography (DIONEX, DX-120 ion chromatograph) and reveals that, even on a neutral surface, oxalate is mineralized in conditions at which the rate of reaction is very slow. In fact, the higher degree of reaction of oxalate takes place with neutral surface charge and neutral pH at which the mineralization is not particularly deep.

For the ozonation of naproxen in the runs reported in Fig. 9, the global extent of mineralization was about 50% in non-catalytic runs at pH 5–7 and reached over 60% using catalyst. The ozonation of carbamazepine allowed a deeper mineralization with 73% TOC reduction after 120 min. In fact, most of the TOC decay takes place during the first 10–20 min where the removal of the more oxidizable compounds takes place. In non-catalytic ozonation, oxalate accounted for as much as 30% of the organic carbon remaining in the

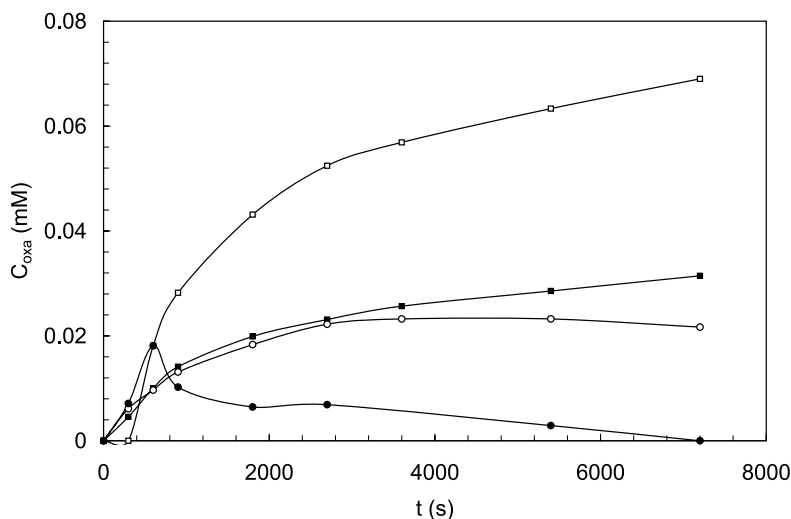


Fig. 9 Concentration of oxalate during the non-catalytic ozonation of naproxen at pH = 5 (□) and the catalytic ozonation on TiO₂ P25 of naproxen at pH = 3 (■), carbamazepine at pH = 3 (○) and carbamazepine at pH = 5 (●). Catalyst loading 1 g/L; initial concentration of naproxen 6.5×10^{-5} M

reaction mixture, in contrast with a maximum of 12% encountered in non-catalytic runs. This pattern reveals that the use of a catalyst favours not only the reactions leading to oxalate but also the mineralization of oxalate itself. In fact, oxalate was not detected in runs performed at pH = 7 with a mineralization degree of about 50%. At pH = 3, at which the surface of P25 is positively charged and may interact with oxalate anion in solution, neither the rate of mineralization nor the removal of oxalate from the solution are particularly high. Therefore, the mineralization of oxalate is not favoured by positive surface charge, a result that seems to exclude a mechanism based on the ion exchange of oxalate.

The results also proved that the rate of ozone decomposition is inhibited by the catalyst over a neutral surface. At pH = 7, the homogeneous rate constant for the ozone self-decomposition is $8.83 \times 10^{-3} \text{ s}^{-1}$ which lowers to $1.27 \times 10^{-3} \text{ s}^{-1}$ in the presence of 1 g/L of P25 TiO₂. The catalytic mineralization rate is a maximum at pH = 5, and the reaction is also inhibited by higher pH values. Anyway, the inhibition effect of increasing the concentration of hydroxide anion is much greater on the mineralization reaction than on ozone decomposition. The best results for the removal of reaction intermediates were obtained for slightly positive surface charge, suggesting that the adsorption of organics on Lewis sites may be the mechanism of the catalytic ozonation of naproxen and carbamazepine. In catalytic runs, the degree of mineralization was not directly linked to the accumulation of low molecular weight carboxylic acids. In all runs, low levels of acetate, formate and other

low weight acids were detected in most cases, but without an accumulation pattern linked to the evolution of TOC. These results point towards a stronger surface interaction with the first ozonation products than with the more oxidized carboxylic acids. The dependence of the degree of mineralization on the rate of adsorption expressed by Eq. 46 was not tested and could be confirmed by experiments performed in conditions at which the integral ozone exposure is not linear with time.

2.5

Applications in the Treatment of Industrial Wastewater

The use of ozone-based technologies for the treatment of pollutants in water has been the focus of attention in the literature during the last few years. Examples of their application as eco-effective alternatives have been presented for several types of contaminants in water, in particular for pharmaceutical residues or PCPs.

Data in scientific publications concerning the use of ozone for industrial wastewater treatments can be found to a lesser extent. As has been mentioned before, ozone is an expensive oxidant and the treatment of industrial or wastewater effluents needs doses higher than those for the treatment of natural waters. In consequence, its use may be limited, but the ability of ozone to mineralize organic matter, alone or in association with other oxidants such as hydrogen peroxide, may be attractive for new developments such as in the reuse of wastewater. Combinations with other oxidation techniques, such as UV irradiation or ultrasonic techniques, can also be of interest due to a higher efficiency and lower cost. The effectiveness of ozone-based technologies has been evaluated in scientific publications for different industrial sectors, such as textiles, petroleum refineries/phenols, pulp and paper, and electroplating wastes.

Recent publications compile and review the studies performed for the treatment of recalcitrant pollutants by the use of AOPs, where possible mechanisms responsible for synergistic action are described [91]. The advantages of combined treatments are the reduction in the time of treatment and higher removal efficiency. In fact, most common approaches have made use of chemical (O_3 or H_2O_2) or photochemical (UV) based processes where the oxidation power for the degradation of organic pollutants can be significantly enhanced.

Table 6 shows a summary of the reviewed literature concerning AOPs applied to the treatment of industrial wastewater effluents. The effectiveness of combined photocatalytic and ozonation processes has been probed for textile effluents [92]. The removal efficiency of phenols from wastewater using a UV/ H_2O_2 / O_3 process ($pH = 7$, $c(H_2O_2) = 10 \text{ mM}$) is complete (100%) within a period of 30 min of treatment [93]. The colouring matter is almost completely eliminated, achieving a high reduction of TOC.

Table 6 Applications of ozone-based processes for the treatment of industrial wastewater

| Industrial activities and others | Pollutants/related pollutants | Treatment | Removal efficiency (%) | Refs. |
|----------------------------------|--|---|-----------------------------|-------|
| Petroleum refineries | Phenols | UV/H ₂ O ₂ /O ₃ | 100% Phenol 58% TOC | [91] |
| Textiles | Colouring matter | TiO ₂ /UV/O ₃ -BAC | 90% Dyes 50% TOC | [93] |
| | Colouring matter | O ₃ and electro-flocculation | > 80% | [94] |
| | PAEs (DMP, DEP, DBP, DEHP) ^a | TiO ₂ /UV/O ₃ -BAC | > 94.9% | [95] |
| | POPs (HCB, PBB003, PBB10, PBB18, PBB52, PBB103) ^b | TiO ₂ /UV/O ₃ -BAC | > 89.3% | [95] |
| Paper | HMW ^c | O ₃ /biological treatment | 80% | [96] |
| | Lignin products (e.g. phenols) | O ₃ /UV | Complete | [97] |
| | Organic load due to starch (e.g. saccharides, carboxylic acids) | | Partial (no data) | |
| Domestic/ other industries | LAS | O ₃ | Complete (aqueous solution) | [98] |
| Agriculture | Pesticides | O ₃ O ₃ /UV O ₃ /H ₂ O ₂ | Complete (aqueous solution) | [99] |
| Pharmacy | Antibiotics Steroid hormones, beta-blockers, X-ray contrast media | O ₃ | > 90% | [100] |

^a Dimethyl phthalate (DMP), diethyl phthalate (DEP), dibutyl phthalate (DBP) and di(2-ethylhexyl) phthalate (DEHP)

^b Hexachlorobenzene (HCB), 4-bromobiphenyl (PBB003), 2,6-dibromobiphenyl (PBB10), 2,2',6-tribromobiphenyl (PBB18), 2,2',5,5'-tetrabromobiphenyl (PBB52) and 2,2',4,5',6-pentabromobiphenyl (PBB103)

^c HMW: organic compounds of high molecular weight

Organic pollutants such as phthalate esters (PAEs) and other POPs in raw water are also efficiently eliminated by various processes which combine the use of catalyst, UV radiation and biological activated carbon, TiO₂/UV/O₃-BAC [94].

The treatment of wastewater effluents generated in the industry of pulp and paper also needs the use of advanced technologies. Pulp mill wastew-

ater contains a significant amount of complex organic compounds of high molecular weight (MW > 1000 Da). It means that the treatment is not feasible by biological methods. The use of ozone-based processes for this type of effluent has demonstrated the capacity of this technology in enhancing the biodegradability, decreasing the toxicity and increasing the removal of organic pollutants from the effluents [95].

The advantage of the combination of a pre-treatment by ozone (dosage of 0.7–0.8 mg O₃/mL wastewater) followed by biological treatment allows the conversion of organic compounds of high molecular weight (HMW) to low molecular weight (LMW), increasing the biodegradability from 5 to 50% [96]. An important factor in this process is the effect of pH. For the treatment of alkaline bleach plant effluent, a superior performance of the ozonation process is under basic pH conditions. It is due to the reaction of organic compounds with molecular ozone and with oxidizing radicals, including the hydroxyl radical, which are effectively formed at high pH. When the paper industry does not employ wood to obtain the pulp and uses recycled paper, the composition of the effluent and pH is not the same, it is less basic.

Another example of the application of advanced technologies using ozone is the treatment of effluents which contain organic compounds arising from the degradation of starch (e.g. saccharides, carboxylic acids), phenolic compounds derived from lignin and smaller amounts of other pollutants that can be persistent in the environment and are detected in fresh water (e.g. surfactants). The studies performed with O₃ and/or UV have shown the utility of this approach. By this procedure, the complete degradation of lignin products and their diminishment has been demonstrated, but the organic load due to starch is not removed. The results obtained in these studies show that toxic or inhibitory compounds (e.g. phenols) are more easily oxidized than the highly biodegradable ones (e.g. glucose, fatty acids) by ozone-based technologies [97].

Linear alkylbenzene sulphonates (LASs) are anionic surfactants which are discharged into wastewaters through different sources (domestic or industrial), reaching aquatic compartments given their wide use. As a reference, in 1995 the world production of LASs was ca. 2.8×10^6 tonnes but now more than 4×10^6 tonnes are consumed globally every year. Few reports can be found on LAS degradation. AOPs have been considered as strong oxidation procedures for the degradation of such organic contaminants. The use of ozonation has been proved as the most efficient approach for degrading the typical LAS mix present in municipal and industrial wastewaters where the typical pH values are slightly basic [98].

Hazardous organic contaminants such as pesticides when discharged into the environment represent a risk for human health and for the ecosystem due to their toxicity and persistence. Several publications have shown the effectiveness of ozone for removing pesticides in aqueous solution [99]. Ozonation appears to be a more efficient technique which can be easily implemented

with UV and/or H₂O₂ for treating wastewater with high organic loads. The efficiency depends, to a great extent, on the nature of the pollutant, and up to now few experiences have been explored and documented for real conditions [99]. AOPs are technologies whose position in the water treatment processes for industry still need to demonstrate levels of reliability and full-scale implementation. For the assessment of the removal efficiency of AOP processes, common procedures are based on the measurement of global parameters (i.e. TOC). The use of techniques such as gas chromatography–mass spectrometry (GC-MS) or liquid chromatography–mass spectrometry (LC-MS) provides analytical information appropriate for further efficiency evaluation and facilitates identification of by-products which can be of environmental concern. The use of toxicity assays in combination with chemical analysis has been considered as a strategic approach for overall assessment [99].

The effluents originating from the pharmaceutical industry can show low biodegradability since they contain active substances. In particular, certain antibiotics, anti-tumour agents and analgesics are neither degradable nor adsorbable on sewage sludge. AOPs applied to remove pharmaceuticals based on the use ozone [100] are able to completely oxidize recalcitrant compounds, rendering them less harmful and forming easily biodegradable components, but also combinations of AOPs have enlarged the possibilities to treat target recalcitrant pollutants [100]. Investigations carried out with antibiotics, steroid hormones, beta-blockers or X-ray contrast media have demonstrated the removal capacity of ozone-based processes, achieving significant elimination of those pharmaceuticals in effluents (> 90%).

2.6

Removal Efficiency of Pharmaceuticals in Wastewater: A Case Study

As has been commented above, it is well established that urban wastewaters, which include domestic and some industrial waters, among others, represent a significant source of contamination with a strongly contaminating effect on natural aquatic systems [101–103]. Even when they are submitted to biological treatment, it has been demonstrated by many studies that multiple organic compounds, such as pharmaceuticals, PCPs, hormones and other disrupting compounds, escape conventional wastewater treatments and some of them are becoming ubiquitous in the environment [104]. The presence of these contaminants in treated waters also endangers their reuse in diverse applications, an aspect which is of special interest since the availability of water of good quality is a critical issue and represents an essential component for sustainable socio-economic development. Consequently, the application of more exhaustive wastewater treatment protocols, including the use of new and improved technologies, the application of wider and integrated quality control strategies comprising chemical, microbiological and toxicological analysis, and the study and development of wastewater reuse strategies are

goals which it is necessary undertake [105]. With this aim, an ambitious programme (TRAGUA) financed by the Spanish Government has been initiated, which attempts to tackle the different aspects involved in the reuse of wastewater coming from sewage treatment plants (STPs). As a part of this programme, results regarding the efficiency of O_3 and O_3/H_2O_2 treatments in the removal of organic contaminants in a municipal wastewater treatment plant (WWTP) effluent are presented.

A suitable analytical methodology was developed in order to obtain an adequate evaluation of the processes. Two LC-MS systems equipped with modern and sensitive mass spectrometers, hybrid triple-quadrupole linear ion trap (QTRAP) and time-of-flight (TOF), were used with this aim. The joint application of both techniques provided very good results in terms of accurate quantification and unequivocal confirmation of the organic pollutants present in the samples. Quantification was performed by LC-QTRAP-MS operating in the selected reaction monitoring (SRM) mode with both positive and negative electrospray ionization, in order to cover a broad range of analytes. Limits of detection reached by the optimized method were between 0.04 and 50 ng L^{-1} , thus guaranteeing an exhaustive evaluation of the samples.

Unequivocal analyte confirmation was provided by LC-TOF-MS analysis, which allows accurate mass measurements of the identified compounds to be obtained with errors lower than 2 ppm. Figure 10 shows as an example the identification by TOF-MS of codeine and acetaminophen, based on the accurate mass of their molecular ions and of their main fragments.

With the application of the developed method, up to 40 compounds were identified in a wastewater effluent after the application of a conventional biological treatment. They include mainly pharmaceuticals of different therapeutic groups, such as analgesics/anti-inflammatories, antibiotics, lipid regulators, beta-blockers, antidepressants, anti-epileptics/psychiatrics, ulcer healing compounds, diuretics and bronchodilators.

The occurrence of many of these compounds has already been reported in environmental waters [106, 107]. Also of interest was the presence of some of their metabolites, such as 1,7-dimethylxanthine (paraxanthine) or fenofibric acid, and especially the metabolites of the antipyretic drug dipyron and its active product 4-methylaminoantipyrine (4-MAA), such as *N*-acetyl-4-aminoantipyrine (4-AAA), *N*-formyl-4-aminoantipyrine (4-FAA) and antipyrine, which were detected at a high level of concentration. Finally, the disinfectant chlorophene and the pesticide diuron completed the group of detected compounds.

All of them are listed in Table 7, where the concentrations found in an effluent sample of a municipal WWTP are also shown. Concentration values ranged from 2 to 6590 ng L^{-1} . The stimulant caffeine, the diuretic hydrochlorothiazide, the beta-blocker atenolol, the analgesic/anti-inflammatory naproxen, the antibiotic ciprofloxacin and the metabolites of dipyron (4-AAA and 4-FAA) were the compounds present at the highest concentration

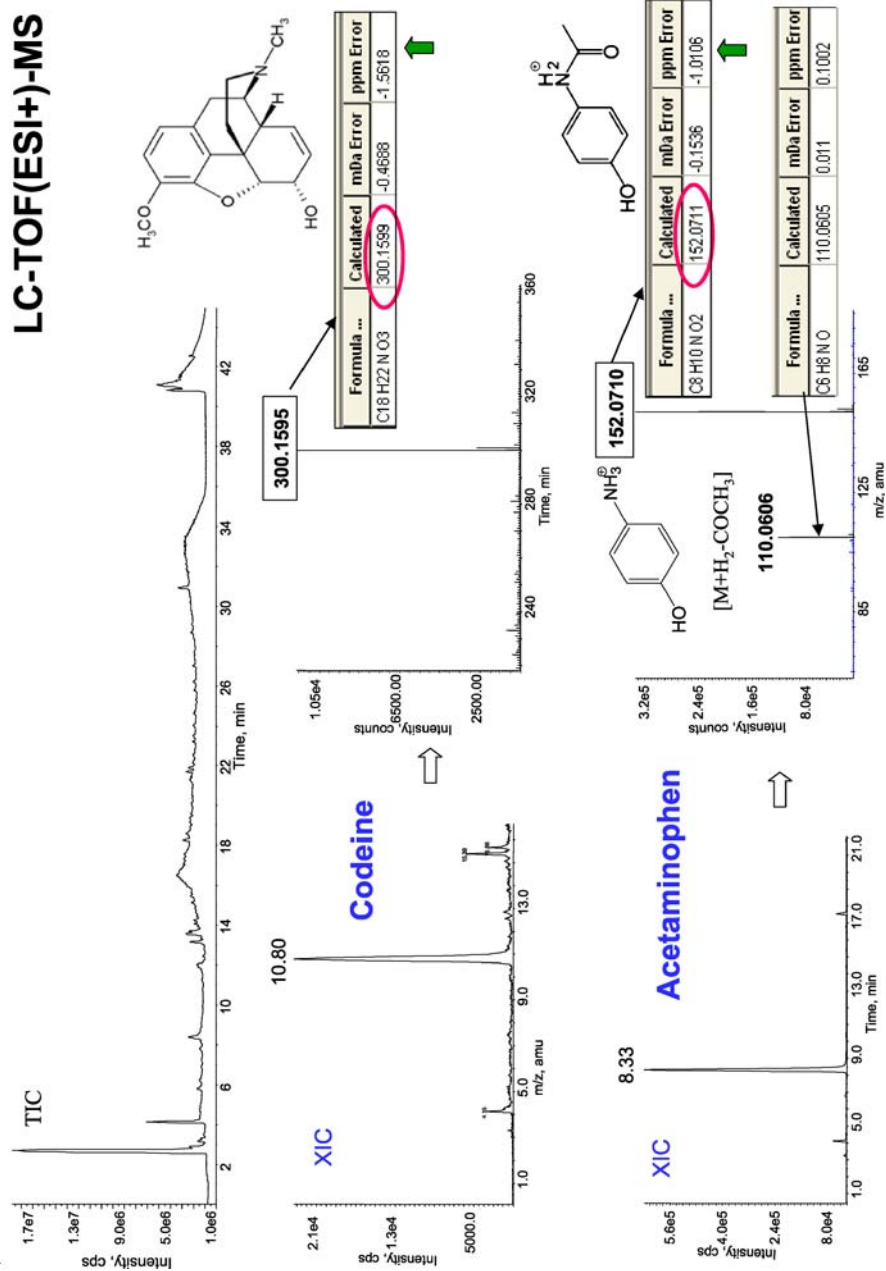


Fig. 10 Example of the identification by TOF-MS of codeine and acetaminophen in an effluent sample based on accurate mass measurements

Table 7 Compounds and concentrations present in a WWTP effluent and their removal efficiency after O₃ and O₃/H₂O₂ treatment

| Compound | Concentration in the effluent (ng L ⁻¹) | Removal efficiency (%) O ₃ | Removal efficiency (%) O ₃ /H ₂ O ₂ |
|---------------------|---|---|--|
| Erythromycin | 341 | 98 | 100 |
| Ciprofloxacin | 2559 | 95 | 99 |
| Sulfamethoxazole | 243 | 97 | 100 |
| Mepivacaine | 2 | 90 | 100 |
| Caffeine | 600 | 93 | 98 |
| Omeprazole | 104 | 98 | 100 |
| Carbamazepine | 140 | 98 | 100 |
| Codeine | 657 | 100 | 100 |
| Ketorolac | 465 | 98 | 100 |
| Paraxanthine | 132 | 87 | 98 |
| Atenolol | 1443 | 99 | 100 |
| Naproxen | 1990 | 98 | 100 |
| Indomethacin | 37 | 100 | 100 |
| Propranolol | 59 | 96 | 100 |
| 4-MAA | 18 | 100 | 100 |
| Diazepam | 5 | 100 | 100 |
| Metoprolol | 53 | 100 | 100 |
| Ranitidine | 336 | 99 | 100 |
| Fluoxetine | 782 | 91 | 100 |
| Trimethoprim | 157 | 98 | 100 |
| Metronidazole | 185 | 100 | 100 |
| 4-FAA | 3191 | 100 | 100 |
| Antipyrine | 17 | 100 | 100 |
| 4-AAA | 6590 | 98 | 100 |
| Ofloxacin | 316 | 97 | 100 |
| Salbutamol | 10 | 100 | 100 |
| Ketoprofen | 590 | 98 | 99 |
| Mefenamic acid | 64 | 96 | 100 |
| Sotalol | 25 | 100 | 100 |
| Terbutaline | 11 | 100 | 100 |
| Fenofibric acid | 165 | 100 | 100 |
| Furosemide | 531 | 98 | 99 |
| Diclofenac | 33 | 100 | 100 |
| Benzafibrate | 61 | 90 | 96 |
| Gemfibrozil | 143 | 88 | 100 |
| Hydrochlorothiazide | 1310 | 96 | 100 |
| Chlorophene | 88 | 86 | 87 |
| Diuron | 9 | 89 | 95 |
| Ibuprofen | 52 | 84 | 96 |

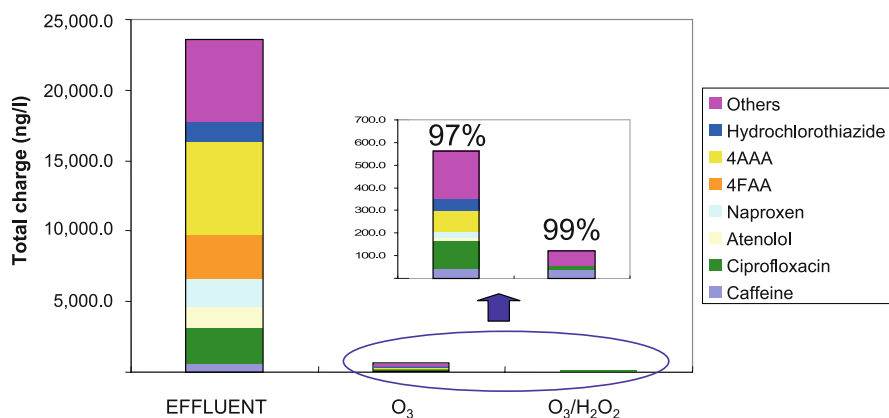


Fig. 11 Total charge of contaminants present in a WWTP effluent before and after the application of O₃ and O₃/H₂O₂ treatments

levels ($> 1 \mu\text{g L}^{-1}$). This group of compounds represents about 75% of the total charge of these contaminants in the effluent, as can be observed in Fig. 11.

The characterized effluent from the secondary clarification of a municipal wastewater treatment facility (Table 7) was submitted to treatment with O₃ and O₃/H₂O₂. The O₃ treatments were carried out at 25 °C in a 5-L stirred tank agitated at 1000 rpm with a four-blade turbine. The gas, a mixture of ozone and oxygen with a 45.9 g Nm⁻³ ozone concentration, was bubbled at a rate of 0.36 Nm³ h⁻¹. During the experiment the pH was in the range 8.04–8.25. The same experimental conditions were maintained in O₃/H₂O₂, but now equal volumes (0.15 mL) of hydrogen peroxide (30% w/v) were injected every 5 min in order to favour pollutant elimination by the radical pathway.

The results obtained demonstrated that ozonation of wastewaters degrades pharmaceuticals with a high efficiency. Removals higher than 90% were reached for most of the target analytes. Only a group of five compounds, gemfibrozil, chlorophene, diuron, ibuprofen and mefenamic acid, yielded lower removal efficiencies, which were higher than 84% in all cases. The combination of ozone and hydrogen peroxide still enhances oxidizing ability, providing almost total elimination of the contaminants in most cases.

Considering the total charge of compounds initially present in the wastewater, a reduction of 97% was observed after O₃ treatment and their almost total elimination (99%) was reached by the application of O₃/H₂O₂, as is shown in Fig. 11. With these results, it can be concluded that both treatments can be considered as promising alternatives for pharmaceuticals and related compounds which persist through conventional biological treatments.

3 Conclusions

Ozone is an efficient oxidant of organic matter but its production is expensive. To optimize the use of ozone it is coupled with coagulation and filtration processes in surface or ground water treatments. It is used alone or coupled with UV in water disinfection processes or it is coupled with other oxidants, energy forms or catalysts in AOPs based on ozone in industrial wastewater treatment.

The process of hydroxyl radical generation from ozone/hydrogen peroxide was modelled in the 1980s, which made it possible to optimize the use of ozone in the elimination of hazardous pollutants, such as pesticides, PAHs, etc. Now the system ozone/hydrogen peroxide is a new choice for water reclamation and potable reuse. The use of the ozone/hydrogen peroxide system as a tertiary treatment of domestic and urban wastewater could provide reclaimed water to use in agriculture or industrial processes. The model of these processes connects the grade of elimination of TOC and ozone doses with the ct -exposure parameter, being the rate of TOC elimination described by a first-order kinetic equation with a kinetic parameter R which is obtained by multiplying the hydroxyl-to-ozone ratio, R_{ct} , and the elimination kinetic constant of TOC, $k_{HO\cdot}$.

The efficiency of homogeneous catalytic ozonation has been reported for several metals, especially iron and manganese. The reaction mechanism involves the oxidation of a reduced form of the metal by ozone, hydroxyl radicals or hydrogen peroxide followed by interaction with the organic compounds. Heterogeneous catalytic ozonation is a complex process whose underlying chemistry is not well known. Several mechanisms have been proposed for describing it that can be classified according to the kind of surface interaction proposed. A Langmuir–Hinshelwood rate expression may account for a reaction between adsorbed organics and oxidized catalytic sites, while an Eley–Rideal model can explain the direct oxidation of an adsorbed organic compound by hydroxyl radicals from the bulk. The ozonation on activated carbon seems to be based on the role of the surface as initiator of the radical chain reactions that transform ozone into radicals.

Other mechanisms exclude adsorption equilibrium and lead to models in which the rate of the catalytic process is not dependent on the concentration of oxidant. An adsorption-limited kinetics seems to be more realistic considering the difficulty of adsorption encountered by organics in aqueous solutions, especially on the surface of oxides. Depending on the pH of the solution, the surface of an oxide may be charged or not. On a neutral surface, the adsorbate must displace water coordination molecules and at basic conditions, Lewis sites would be inhibited by the hydroxide anion. On oxides, such as titanium dioxide, the reaction is probably better described by an interaction between Lewis acid sites and organic molecules, with an optimum mineralization rate obtained in slightly acidic conditions.

The ozonation reaction of individual compounds showed that the ozonation starts with a rapid mineralization period followed by a slow decay of the organic carbon associated with the accumulation of refractory compounds. Some other circumstances complicate the modelling and description of a catalytic ozonation process. For example, the distribution of reaction products markedly differs from that encountered in non-catalytic reactions. Understanding the role of catalyst in the inhibition of the ozone decomposition reaction and the determination of values of the hydroxyl-to-ozone ratio, R_{ct} , a parameter that may change during the reaction and that the catalyst can modify, are additional difficulties.

Acknowledgements The authors wish to express their gratitude to the Ministry of Education of Spain (Contracts CTM2005-03080/TECNO, CTM2004-06265-C03-03 (EVITA) and CONSOLIDER-INGENIO 2010 CSD2006-00044), the Dirección General de Universidades e Investigación de la Comunidad de Madrid under Contract No. PAMB-000395-0505 and the research network from Comunidad de Madrid REMTAVARES Ref. 0505/AMB-0395.

References

1. Andreozzi R, Caprio V, Ermellino I, Insola A, Tufano V (1996) *Ind Eng Chem Res* 35:1467–1471
2. Rischbieter E, Stein H, Shumpe A (2000) *J Chem Eng Data* 45:338–340
3. Roth JA, Sullivan DE (1981) *Ind Eng Chem Fundam* 20:137–140
4. Sotelo JL, Beltran FJ, Benitez FJ, Beltran-Heredia J (1989) *Water Res* 23:1239–1246
5. Beltran FJ, García-Araya JF, Encinar JM (1997) *Ozone Sci Eng* 19:281–296
6. Charpentier JC (1981) Mass-transfer rates in gas–liquid absorbers and reactors. In: Drew TB, Coker GR, Hoopes HW Jr, Vermeulen T (eds) *Advances in chemical engineering*, vol 11. Academic, New York, pp 3–133
7. Danckwerts PV (1970) *Gas–liquid reactions*. McGraw-Hill, New York, p 113
8. Onda K, Sada E, Kobayashi T, Fujine M (1979) *Chem Eng Sci* 25:761–768
9. Beltran FJ, Encinar JM, García-Araya JF, Alonso MA (1992) *Ozone Sci Eng* 14:303–327
10. Poling BE, Prausnitz JM, O’Connell JP (2001) *The properties of gases and liquids*. McGraw-Hill, New York, p 25
11. Beltrán FJ (2004) *Ozone reaction kinetics for water and wastewater systems*. CRC, Boca Raton, pp 70–87
12. Chalmet S, Ruiz-López M (2006) *J Chem Phys* 124:1945
13. Buhler RE, Staehelin S, Hoigné J (1984) *J Phys Chem* 88:2560–2564
14. Staehelin S, Buhler RE, Hoigné J (1984) *J Phys Chem* 88:5999–6004
15. Tomiyasu H, Fukutomi H, Gordon G (1985) *Inorg Chem* 24:2962–2966
16. Hoigné J (1998) Chemistry of aqueous ozone and transformation of pollutants by ozone and advanced oxidation processes. In: *Handbook of environmental chemistry*, vol 5, part C. Quality and treatment of drinking water II. Springer, Berlin
17. Staehelin S, Hoigné J (1983) *Vom Wasser* 61:337–348
18. Kasprzyk-Hordern B, Ziolk M, Nawrocki J (2003) *Appl Catal B Environ* 46:639–669
19. Lin J, Kawai A, Nakajima T (2002) *Appl Catal B Environ* 39:157–165
20. Logemann FP, Annee JHJ (1997) *Water Sci Technol* 35:353–360

21. Sánchez-Polo M, von Gunten U, Rivera-Utrilla J (2005) *Water Res* 39:3189–3198
22. Rivera-Utrilla J, Sánchez-Polo M, Mondaca MA, Zaror CA (2002) *J Chem Technol Biotechnol* 77:883–890
23. von Gunten U (2003) *Water Res* 37:1443–1467
24. Elovitz MS, von Gunten U (1999) *Ozone Sci Eng* 21:239–260
25. Rosal R, Rodríguez A, Zerhouni M (2006) *Appl Catal A Gen* 305:169–175
26. Beenackers AACM, van Swaaij WPM (1993) *Chem Eng Sci* 48:3109–3139
27. Acero JL, von Gunten U (2001) *J Am Water Works Assoc* 93:99–100
28. Buffle MO, Schumacher J, Meylan S, Jekel M, Gunten U (2006) *Ozone Sci Eng* 28:245–249
29. Buffle MO, Schumacher J, Salhi E, Jekel M, Gunten U (2006) *Water Res* 40:1884–1894
30. Langlais B, Reckhow DA, Brink DR (1991) *Ozone in water treatment: application and engineering*. AWWA Research Foundation and Lewis, Denver
31. Sonntag C (2007) *Water Sci Technol* 55:19–23
32. Barreto R, Gray KA, Andres K (1995) *Water Res* 29:1243–1248
33. Albarran G, Schuler RH (2005) *J Phys Chem A* 109:9363–9370
34. Palmisano G, Addamo M, Augugliaro V, Caronna T, Paola A, García E, Loddo V, Marci G, Palmisano L, Schiavello M (2007) *Catal Today* 122:118–127
35. Fang X, Schuchmann HP, Sonntag J (2000) *J Chem Soc Perkin Trans 2* 1391–1398
36. Legube B, Karpel N (1999) *Catal Today* 53:61–72
37. Sallanko J, Lakso E, Röpölinen J (2006) *Ozone Sci Eng* 28:269–273
38. Langlais B, Reckhow DA, Brink DR (eds) (1991) *Ozone in drinking water treatment: application and engineering*. AWWARF and Lewis, Boca Raton
39. Ramírez F (2005) *Tratamiento de desinfección de agua potable*. Canal de Isabel II, Madrid, p 9
40. Viraraghavan T, Subramanian KS, Aruldoss JA (1999) *Water Sci Technol* 40:69–76
41. Nishimura T, Umetsu Y (2001) *Hydrometallurgy* 62:83–92
42. Kim MJ, Nriagu J (2000) *Sci Total Environ* 247:71–79
43. von Gunten U (2003) *Water Res* 37:1469–1487
44. USEPA (1989) *National primary drinking water regulations: final rules* 54:27485–27541
45. von Gunten U, Elovitz MS, Kaiser HP (1999) *J Water Supply Aqua* 48:250
46. Do-Quang Z, Roustan M, Duguet JP (2000) *Ozone Sci Eng* 22:99–111
47. Xu P, Janex ML, Savoye P, Cockx A, Lazarova V (2002) *Water Res* 36:1043–1055
48. Camel V, Bermond A (1998) *Water Res* 32:3280–3222
49. Rice RP (1999) *Ozone Sci Eng* 21:99–118
50. Larocque RL (1999) *Ozone Sci Eng* 21:119–125
51. Matsumoto N, Watanabe K (1999) *Ozone Sci Eng* 21:127–138
52. Kruithof CJ, Masschelin W (1999) *Ozone Sci Eng* 21:139–152
53. Paulose J, Langlais B (1999) *Ozone Sci Eng* 21:153–162
54. Böhme A (1999) *Ozone Sci Eng* 21:163–176
55. Pollo I (1999) *Ozone Sci Eng* 21:177–186
56. Geering F (1999) *Ozone Sci Eng* 21:1187–1200
57. Lowndes R (1999) *Ozone Sci Eng* 21:201–205
58. Haag WR, Hoigné J (1985) *Chemosphere* 14:1569–1671
59. Hoigné J (1997) *Water Sci Technol* 35:1–8
60. Yurteri C, Gurol DM (1988) *Ozone Sci Eng* 10:277–290
61. Glaze WH, Kang J-W (1989) *Ind Eng Chem Res* 28:1573–1580
62. Glaze WH, Kang J-W (1989) *Ind Eng Chem Res* 28:1580–1587
63. Beltran FJ, Rivas J, Alvarez PM, Alonso MA (1999) *Ind Eng Chem Res* 38:4189–4199

64. Legube B (2003) Ozonation by-products. In: Handbook of environmental chemistry, vol 5, part G. Springer, Berlin, pp 95–116
65. Andreozzi R, Insola A, Caprio V, D'Amore MG (1992) *Water Res* 26:917–925
66. Andreozzi R, Marotta R, Sanchirico R (2000) *J Chem Technol Biotechnol* 75:59–65
67. Beltrán FJ, Rivas FJ, Montero R (2002) *Appl Catal B Environ* 39:221–231
68. Beltrán FJ, Rivas FJ, Montero R (2003) *J Chem Technol Biotechnol* 78:1225–1233
69. Beltrán FJ, Rivas FJ, Montero R (2005) *Water Res* 39:3553–3564
70. Rivera-Utrilla J, Sánchez-Polo M (2002) *Appl Catal B Environ* 39:319–329
71. Faria PCC, Órfao JJM, Pereira MFR (2005) *Water Res* 39:1461–1470
72. Andreozzi R, Casale MS, Marotta R, Pinto G, Pollio A (2000) *Water Res* 34:4419–4429
73. Gracia R, Cortes S, Sarasa J, Ormad P, Ovelleiro JL (2000) *Water Res* 34:1525–1532
74. Ma J, Graham NJD (1999) *Water Res* 33:785–793
75. Lin J, Nakajima T, Jomoto T, Hiraiwa K (1999) *Ozone Sci Eng* 21:241–247
76. Karpel N, Delouane B, Legube B, Luck F (1999) *Ozone Sci Eng* 21:261–276
77. Fu H, Karpel N, Legube B (2002) *New J Chem* 26:1662–1666
78. Hewes CG, Davinson RR (1972) *Water AICChE Symp Ser* 70:69–71
79. Gracia R, Aragües JL, Cortés S, Ovelleiro JL (1996) *Ozone Sci Eng* 18:195–208
80. Piera E, Calpe JC, Brillas E, Domenech X, Peral J (2000) *Appl Catal B Environ* 27:169–177
81. Nowell LH, Hoigné J (1987) Interaction of iron(II) and other transition metals with aqueous ozone, 8th Ozone World Congress, Zurich, September 1987, p E80
82. Neyens E, Baeyens JH (2003) *J Hazard Mater* B29:33–50
83. Pines DS, Reckhow DA (2002) *Environ Sci Technol* 36:4046–4051
84. Dhandapani B, Oyama ST (1997) *Appl Catal B Environ* 11:129–166
85. Bulanin KM, Lavalley JC, Tsyganenko AA (1995) *Colloids Surf A* 101:153–158
86. Fernandez P, Nieves FJDL, Malato S (2000) *J Colloid Interface Sci* 227:510–516
87. Zhaobin W, Xienian G, Sham EL, Grange P, Delmon B (1990) *Appl Catal* 63:305–317
88. Kasprzyk-Hordern B (2004) *Adv Colloid Interface Sci* 110:19–48
89. Beltrán FJ, Rivas FJ, Montero R (2004) *Appl Catal B Environ* 47:101–109
90. Vannice MA (2007) *Catal Today* 123:18–22
91. Agustina TE, Ang HM, Vareek VK (2005) *J Photochem Photobiol C Photochem Rev* 6:264–273
92. Moraes SG, Freire RS, Duran N (2000) *Chemosphere* 40:369–373
93. Kusic H, Koprivanac N, Bozic AL (2006) *Chem Eng J* 123:127–137
94. Ciardelli G, Ranieri N (2001) *Water Res* 35:567–572
95. Li L, Zhu W, Zhang P, Zhang Q, Zhang Z (2006) *J Hazard Mater* 128:145–149
96. Bijan L, Mohsein M (2005) *Water Res* 39:3763–3772
97. Amat AM, Arques A, Miranda MA, López F (2005) *Chemosphere* 60:1111–1117
98. Fernández J, Riu J, García-Calvo E, Rodríguez A, Fernández-Alba AR, Barceló D (2004) *Talanta* 64:69–79
99. Chiron S, Fernández-Alba AR, Rodríguez A, García-Calvo E (2000) *Water Res* 34:366–377
100. Hernando MD, Petrovic M, Radjenovic J, Fernández-Alba AR, Barceló D (2007) Removal of pharmaceuticals by advanced treatment technologies. In: Petrovic M, Barceló D (eds) *Analysis, fate and removal of pharmaceuticals in the water cycle*. Elsevier Science Ltd., Oxford, UK
101. Gómez MJ, Martínez Bueno MJ, Lacorte S, Fernández-Alba AR, Agüera A (2007) *Chemosphere* 66:993–1002
102. Hernando MD, Mezcuca M, Fernández-Alba AR, Barceló D (2006) *Talanta* 69:334–342
103. Zuccato E, Castiglioni S, Fanelli RE (2005) *J Hazard Mater* 122:205–209

104. Carballa M, Omil F, Lema JM, Llompart M, García-Jares C, Rodríguez I, Gómez M, Ternes TA (2004) *Water Res* 38:2918–2926
105. Hernando MD, Ferrer I, Agüera A, Fernández-Alba AR (2004) In: Barcelo D (ed) *Emerging organic pollutants in waste waters and sludge*. Springer, Berlin, pp 53–77
106. Bendz D, Paxeus NA, Ginn TR, Loge FJ (2005) *J Hazard Mater* 122:195–204
107. Bound JP, Voulvoulis N (2004) *Chemosphere* 56:1143–1155